ELECTROCHEMICAL EVALUATION OF TCO MODIFICATIONS USING SUBSTITUTED FERROCENES

by

Saehan Park

A Thesis Submitted to the Faculty of the

DEPARTMENT OF CHEMISTRY AND BIOCHEMISTRY

In Partial Fulfillment of the Requirements

For the Degree of

MASTER OF SCIENCE
WITH A MAJOR IN CHEMISTRY

In the Graduate College

THE UNIVERSITY OF ARIZONA

2 0 1 2

STATEMENT BY AUTHOR

This thesis has been submitted in partial fulfillment of requirements for an advanced degree at The University of Arizona and is deposited in the University Library to be made available to borrowers under rules of the Library.

Brief quotations from this thesis are allowable without special permission, provided that accurate acknowledgement of source is made. Requests for permission for extended quotation from or reproduction of this manuscript in whole or in part may be granted by the head of the major department or the Dean of the Graduate College when in his or her judgment the proposed use of the material is in the interests of scholarship. In all other instances, however, permission must be obtained from the author.

SIGNED: Saehan Park

APPROVAL BY THESIS DIRECTOR

This thesis has been approved on the date shown below:

_____ _____ 08/08/2012 _____

S. Scott Saavedra — Date

Professor of Chemistry and Biochemistry

TABLE OF CONTENTS

TABLE OF CONTENTS - Continued

TABLE OF CONTENTS - Continued

TABLE OF CONTENTS - Continued

LIST OF FIGURES

LIST OF FIGURES - Continued

LIST OF FIGURES - Continued

LIST OF TABLES

ABSTRACT

The modifications of transparent conductive oxides (TCOs) have been studied using an electrochemical evaluation technique (cyclic voltammetry (CV)). Substituted ferrocenes were chemically adsorbed onto the surface of indium tin oxide (ITO) and indium zinc oxide (IZO). The electroactive surface coverage, the redox potential, and the charge transfer rate of the adsorbed modifiers were evaluated using CV. The highest electroactive surface coverage was produced by ferrocene phosphonic acid while ferrocene acetic acid showed the fastest charge transfer rate.

The charge transfers with the modified electrodes were evaluated in the presence of a solution electroactive probe. The charge transfer rate of the solution probe was enhanced with the modified electrodes compared to the charge transfer rate measured with unmodified electrodes. Even though the cause of the enhancement in the charge transfer rate is not clear, the results suggest that the modification of TCO may improve the charge collection efficiency of TCO, which is desirable for the application of TCO in devices such as organic photovoltaic cells.

1. BACKGROUND/MOTIVATION AND THE PLAN OF STUDY

1.1 Organic solar cell and efficiency enhancement

1.1.1 Introduction to organic solar cells

Solar cells (photovoltaics) are designed to convert sunlight energy into electrical energy. In photovoltaics, electron-hole pairs are created in a semiconductor by absorption of photons, and electric current can be generated when the pairs are separated into free charge carriers (electrons and holes) and travel in opposite directions in the circuit.[5-7] Currently, the predominant materials used in solar cells are inorganic, especially silicon-based semiconductors. However, the flexibility and low production cost expected for organic materials via diverse synthetic methods have led to great interest in organic semiconductor-based photovoltaics. Figure 1.1 illustrates the structure of a normal planar heterojunction organic photovoltaic cell and its operation.[1, 8, 9]

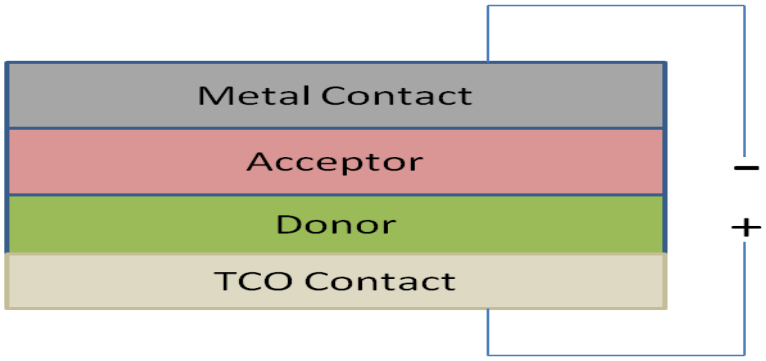

(a)

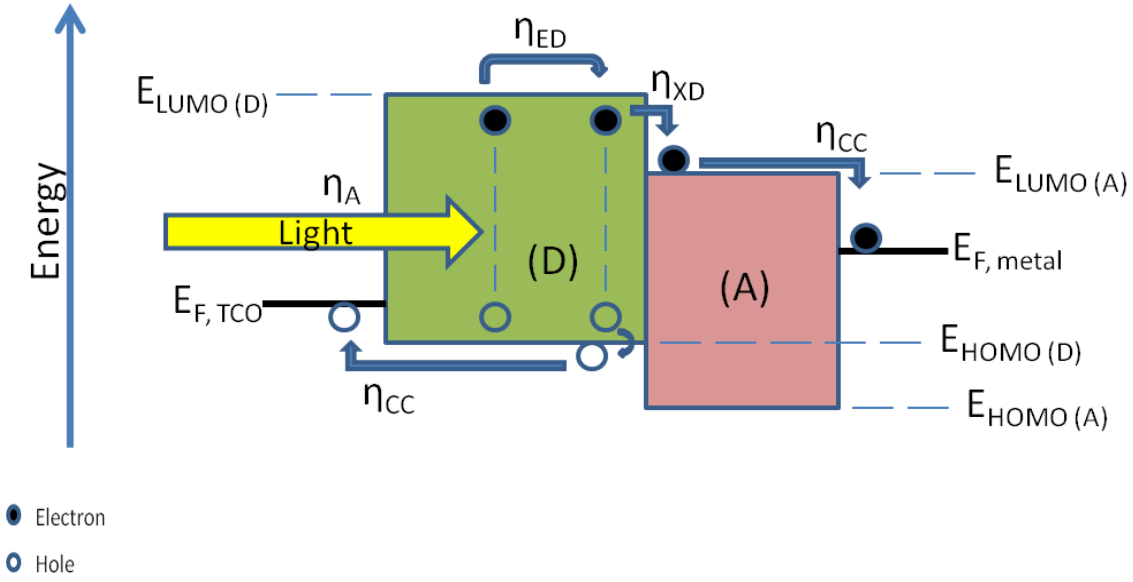

η_A: Photon absorption efficiency. η_{ED}: Exciton diffusion efficiency. η_{XD}: Exciton dissociation efficiency.
η_{CC}: Charge collection efficiency. (D): Donor. (A): Acceptor. E_F: Fermi level.
E_{HOMO}: Energy of highest occupied molecular orbital. E_{LUMO}: Energy of lowest unoccupied molecular orbital.

(b)

Figure 1.1 (a) Structure of a normal planar heterojunction OPV. (b) Illustration of the normal planar heterojunction OPV operation.[1] (Adapted from Ref. 1).

In spite of the advantages, the low conversion efficiency of organic photovoltaics ($\eta < 11\%$) compared to inorganic devices ($\eta = \sim 20\%$) have limited their commercial use.[10-12] In comparison with inorganic semiconductors, organic semiconductors generally have poor (orders of magnitudes lower) charge carrier mobility.[13] Additionally, organic semiconductors produce tightly bound (Frenkel) excitons that have exciton binding energy of 0.1 – 1eV whereas inorganic semiconductors produce weakly bound (Mott-Wannier) excitons that have exciton binding energy of < 0.01 mV.[10, 14, 15] These features contribute to the low efficiency of organic photovoltaics (OPVs). The external quantum efficiency (η_{EQE}) of an OPV, which is the number of electrons flowing in the external circuit per photon incident on the cell, can be described with the following equation.[1]

$$\eta_{EQE} = \eta_A \times \eta_{ED} \times \eta_{XD} \times \eta_{CC} \quad (1.1)$$

where η_A, η_{ED}, η_{XD}, and η_{CC} are the quantum efficiencies of exciton generation by photon absorption, exciton diffusion, exciton dissociation, and charge collection of preferred free carriers at the electrodes. While different researchers and groups have been working on improving individual

efficiencies, we focused on investigating the charge collection efficiency. Especially, the charge collection at transparent conductive oxide (TCO) electrode was thought to be problematic due to the shortcomings of TCO and of its interface that are described in Section 1.1.2. This work focuses on the charge collection efficiency at the TCO/organic interface. More specifically, the rate of heterogeneous charge transfer at the oxide/organic interface. Modifications of TCOs have been performed to see if they have a potential to improve η_{CC}, which may lead to the enhancement of the overall quantum efficiency.

1.1.2 Transparent conductive oxide electrode modification

Transparent conductive oxide thin film electrodes have been used in optoelectric devices such as organic light emitting devices (OLEDs) and OPVs because TCOs are both optically transparent and electrically conductive.[16] In order for the OPV shown in Figure 1.1 to generate current, charge transfers are required at interfaces, including the interface between the TCO and the donor layer. However, the polar hydrophilic surfaces of TCOs are generally incompatible with a nonpolar layer of organic species and are a cause of poor stability and high charge transfer resistance.[16]

Additionally, surfaces of TCOs are often electrically heterogeneous, which may result in local variation of the charge transfer rate at the interface.[8, 17] Modifications of the surface of TCOs have been introduced to resolve the problems. Silanizations and chemisorptions of molecules with hydrophilic functional groups on TCO surfaces have been widely used as modification strategies.[18-20] Acidic functional groups, such as carboxylic acids and phosphonic acids, are often used in the chemisorption strategy,[19] and power conversion efficiency improvements in OLED and OPV have been observed.[21, 22]

1.2 Evaluation of modified TCOs

1.2.1 Investigation of charge transfer rate variation by TCO modifications with different modifiers

Motivated by the positive impact of the TCO modification mentioned in the previous section, modified TCOs with different modifiers were investigated. The structures of modifiers used are depicted in Figure 1.2. All modifiers used were composed of a binding group and a terminal group. Binding groups were acidic functional groups that can bind to metal oxide surfaces: acetic acid (AA), boronic acid (BA), carboxylic acid (CA),

hydroxamic acid (HA), phosphonic acid (PA), and sulfonic acid (SA).[19, 23-26] When they are bound to the TCOs, the electronic states of the surface can be changed.[27] Considering the compatibility with the organic active layers in an OPV, an organic moiety is desired for the terminal group. An organic redox active molecule, ferrocene (Fc), was used as the terminal group for all modifiers, so that the impact of different binding groups could be electrochemically investigated.

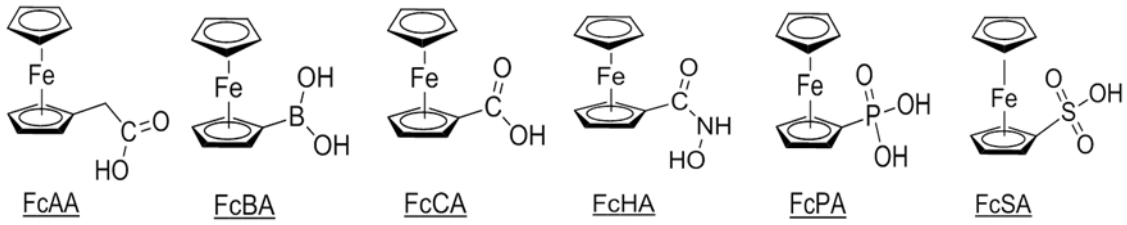

Figure 1.2 Ferrocene derivatives with different acidic functional groups.

An electroactive molecular probe was used to evaluate modified TCOs. The charge transfer between the dissolved electroactive probe and a TCO is a simplified analogue of the charge transfer from the donor layer to TCO in Figure 1.1. The model system allows us to conveniently measure and compare the charge transfer rate at modified and non-modified TCO surfaces. Assuming that the improvement of the charge collection efficiency

(η_{CC}) corresponds to the enhancement of the charge transfer rate, the impact of the TCO modification on η_{CC} can be estimated. It was assumed that the charge transfer rate measured from a redox reaction that include both charge injection and extraction will equate to a rate of the one-directional hole collection. The solution probe used in the study is Fc, which has useful characteristics for being a model probe that are described in Section 1.2.2.

A limit of the model system is that the charge recombination effect is not considered. In a complete cell, the charge recombination may occur during the charge transport through the organic active layers and reduces η_{CC},[28, 29] which is not expected in the model system with a solution probe. Additionally, in the model system, the charge transfer rate is investigated by applying potential to the electrode, which modulates the energy level of the electrode and artificially aligns it with the highest occupied molecular orbital (HOMO) level of the solution probe (Fc). However, in an OPV, the energy level of the electrode is fixed, so an energy level offset between the donor and the electrode may exist. The energy level offset can affect the charge collection rate, and could potentially vary the charge collection efficiency at the electrode.

The electroactivity of a TCO surface may be altered via adsorption of modifiers, which can lead to a change in the charge transfer rate of the solution probe at the interface. The change in the charge transfer rate can be described using the Randles circuit illustrated in Figure 1.3, which is an equivalent electric circuit proposed for the interface between electroactive species in solution and an electrode, where R_s, C_{dl}, R_{ct}, and Z_w are solution resistance, double layer capacitance, charge transfer resistance, and Warburg impedance (impedance representing diffusion of electroactive species) respectively.[30-32] When the surface electroactivity of a TCO is altered via adsorption of modifiers, it changes the value of R_{ct}, which is inversely proportional to the standard rate constant (k°) of the charge transfer reaction for the electroactive species.[33, 34] The value of R_{ct} can be varied with each individual modifier if each modifier generates a different degree of electroactivation.

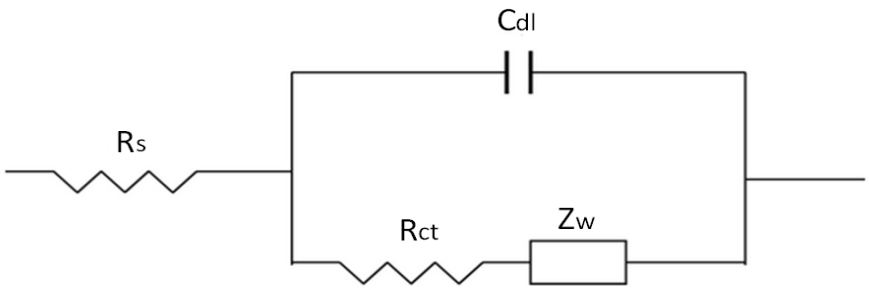

Figure 1.3 An equivalent circuit for the electrode / electroactive species interface.

It is hypothesized that the electroactive surface coverage of the modifier is correlated with the degree of electroactivation of the surface. This hypothesis was developed with the following assumptions: i) electroinactive species covers the intrinsically electroactive TCO surface, ii) the electroinactive species can be removed via adsorption of modifiers, and iii) all electroactive sites are occupied by modifiers. If the assumptions and the hypothesis are valid, the electroactive surface coverage measured for each modifier will be correlated to the charge transfer rate measured with the modified TCO.

Assuming that every oxygen in each acidic functional group can be involved in forming a metal-oxygen bond (metal from TCO surface), FcPA and FcSA are expected to have tridentate binding modes while other

modifiers have bidentate binding modes. Thus, FcPA and FcSA are expected to be more robustly bound on TCO surfaces than others. Additionally, if the robust binding can promote more molecules to be bound on the surface, the charge transfer rate of the solution probe can be enhanced greater with TCOs modified with FcPA or FcSA than other modifiers.

1.2.2 Ferrocene as an electroactive molecular probe

As shown in Figure 1.4, ferrocene has two cyclopentadienyl (C_p) rings that coordinate η^5 to one Fe(II) cation, and the overall complex is neutral.[35] Even though there are some rotational variations suggested, based on the energy of the conformation, it is generally believed that the two C_p rings are staggered to each other, resulting in D_{5d} symmetry for this molecule.[36-38] The average Fe–C distance is 2.045 Å and the C–C distance is 1.403 Å.[36] Ferrocene is highly soluble in organic solvents while insoluble in aqueous solvents, and it has reaction characteristics of aromatic compounds.[35] Ferrocene has been extensively studied, and numerous reports have shown that an oxidation of ferrocene $Fe(II)(C_5H_5)_2$ to ferrocenium cation $Fe(III)(C_5H_5)_2^+$ and the reverse reaction (reduction) can be electrochemically accomplished in a variety of organic media.[39-45] In addition to the well

known one electron transfer redox reaction, the highest occupied molecular orbital (HOMO) level of ferrocene (4.8 eV below the vacuum level)[46] is comparable to common donor materials in OPVs such as copper phthalocyanine (4.8 ~ 5.1 eV)[47], poly(3-hexylthiophene) (4.9 eV)[48], and poly(3,4-ethylenedioxythiophene):poly(styrenesulfonate) (5.2 eV)[49], so ferrocene can be a model.

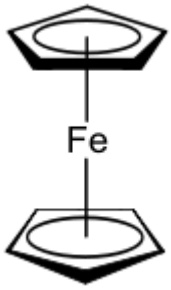

Figure 1.4 The structure of ferrocene.

1.2.3 Analytical technique

Cyclic voltammetry (CV) was used for the electrochemical evaluation of the dissolved and adsorbed molecules in this study. CV is one of the most widely used techniques for investigating surface charge transfer processes and does not require highly expensive or complicated instrumentation.[50, 51] In CV, current is measured as the function of a controlled potential sweep,

and thermodynamic and kinetic parameters, such as the redox potential and charge transfer rate coefficient of a surface charge transfer reaction, can be determined. Additionally, an electroactive surface coverage of adsorbed molecules on a TCO electrode can be determined.[52]

A limit of the technique is that it does not give any structural information of the molecule. For instance, the molecular binding orientation, which can be correlated with the surface coverage, cannot directly be investigated by CV. Additionally, if a peak observed in a voltammogram consists of several components, it is difficult to differentiate the effect of each component. The individual components can represent the same molecules in different binding sites or with different binding modes. However, the analysis of the voltammogram can only give one representative value of redox potential or charge transfer rate for the whole composition. Details of the data analysis are described in Appendix A (for dissolved molecules) and B (for adsorbed molecules).

1.3 Overview of the experiments

This research is focused on evaluating charge transfer reactions at TCO interfaces corresponding to the surface modifications via

chemisorptions of various acidic functional groups. The remainder of the document is divided into two parts:

I) In Chapter 2, modifications of the most widely used TCO, indium tin oxide (ITO), have been studied. Cyclic voltammetry of molecules controlled by diffusion was conducted on the dissolved molecules to investigate their electrochemical characteristics, redox potential and charge transfer rate, before binding to the ITO surface. Subsequent electrochemical evaluation on adsorbed modifiers was performed to investigate adsorption coverages, redox potentials, and charge transfer rates of the different modifiers when tethered to ITO. Finally, charge transfers with modified electrodes were evaluated in the presence of a solution redox probe to determine if the modifications have a noticeable impact on the charge transfer reaction of the solution probe.

II) In Chapter 3, indium zinc oxide (IZO), a candidate for replacing ITO, has been studied. The charge transfer rate of a solution redox probe with unmodified IZO was measured using cyclic vomtammetry to compare the intrinsic electrochemical property of IZO and ITO. Electrochemical evaluation of adsorbed layers of FcCA and FcPA was performed to investigate how adsorption coverages, redox potentials, and charge transfer

rates of the modifiers are changed when tethered to IZO in comparison with ITO. The charge transfer rate of a solution redox probe was also measured with FcCA and FcPA modified IZO to see if the modifiers have the same impact on IZO compared to ITO. Additionally, nano-structured IZO has been tested for adsorption of FcPA. The electroactive surface coverage and the charge transfer rate of FcPA on nano-structured IZO were evaluated to see if controlling the surface geometry of IZO can generate an enhancement of the electrochemical characteristics.

2. EVALUATION OF SUBSTITUTED FERROCENE MODIFIERS ON ITO

2.1 Introduction

2.1.1 Introduction to ITO

Indium tin oxide (ITO) is a tin-doped indium oxide with typical wt. % ratio (oxide weight ratio or In-Sn atomic ratio) of 90:10. Various solution and thermal processes are available to produce ITO thin films and coatings.[53] Sputtering techniques are widely used for depositing ITO films.[54] An ITO layer commonly has a conductivity of $(3 – 5) \times 10^3$ S/cm and an optical transmittance of 85 – 90% in the visible spectral region when deposited as a thin film.[55] The electrical conductivity of ITO is due to interstitial tin dopants and oxygen defects in the indium oxide lattice, which produce electron rich states near the conduction band of indium oxide (Figure 2.1).[2] The bandgap of ITO has been reported in a range from 3.5 to 4.06 eV.[2, 56] ITO has been used in a variety of devices such as plasma displays and flat panel displays, and it is one of the most commonly used TCOs in photovoltaics.[53]

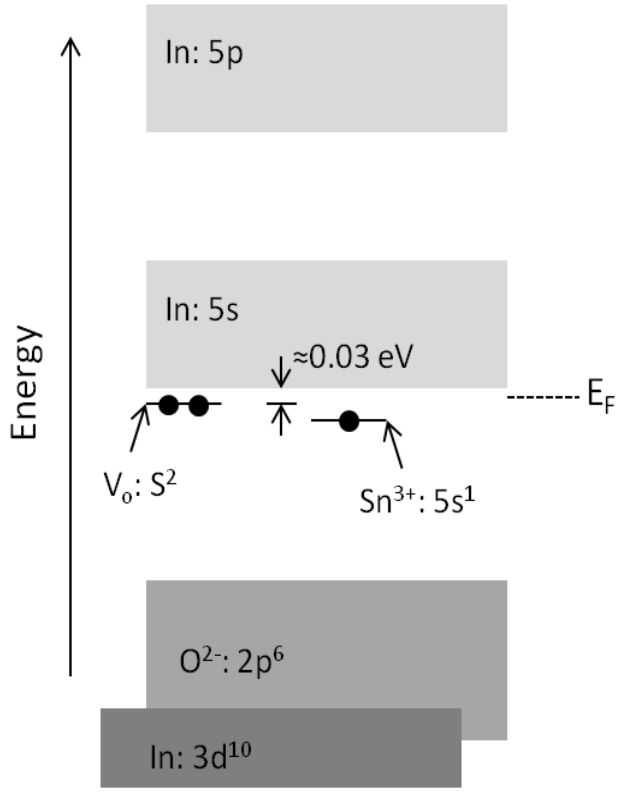

Figure 2.1 Proposed band structure of ITO film. Oxygen defects and tin dopants contribute to electron density around the conduction band of the indium oxide.[2] (Adapted from Ref. 2).

The composition of ITO surfaces has been studied, and X-ray photoelectron spectroscopy (XPS) results suggest that various oxides and hydroxides are formed in the surface region as shown in Figure 2.2.[3] Additionally, it has been observed by using atomic force microscopy (AFM)

and conductive tip AFM that the surface of ITO is electrically heterogeneous, meaning that it is composed of electroactive and non-electroactive regions.[17, 57] Indium hydroxides, $In(OH)_3$, formed from the disrupted ITO lattice, remained physisorbed at the surface after cleaning[3] and may be a reason for the electroinactivity.[22, 58] Even though ITO has relatively good conductivity and optical transmittance, its electrochemical heterogeneity in near surface may reduce device performance of OPVs. Using kinetic Monte Carlo simulations, Zacher and Armstrong demonstrated that the charge collection efficiency could be reduced when electrodes are partially blocked.[59] Blocking of the electrode was modeled as ratios of electroactive sites to total sites.

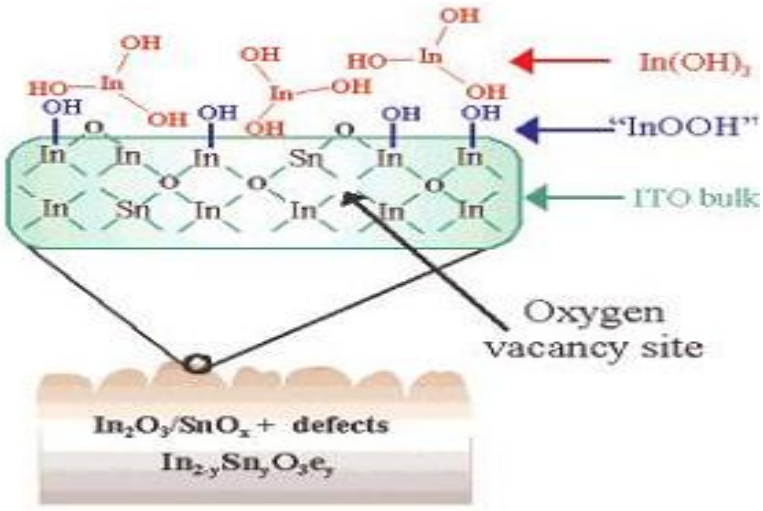

Figure 2.2 A representation of the complex composition of the ITO surface region.[3] (Adapted from Ref. 3).

2.1.2 Modification of ITO

As discussed in the above section, ITO is a partially blocked (electroinactive) electrode that consists of electrically active regions and non-active regions due to the heterogeneous structure at the surface.[57] A simple relationship is often used for describing the charge transfer rate of a partially blocked electrode.[22, 60-63]

$$k^\circ = k^\circ_0(1 - \theta) \qquad (2.1)$$

where k° is the charge transfer rate constant measured with a partially blocked electrode, $k°_0$ is the charge transfer rate constant if the electrode is 100% electroactive, and θ is the fractional area of the electroinactive region. From this relationship, an increse in the fractional area of the electroactive region can be expected when an enhancement of k° is observed. Assming the ITO surface covered with ($In(OH)_3$) is a reason for the electroinactivity, if k° of a redox probe is increased after a modification of ITO, then removal of the $In(OH)_3$ can be suggested.

For metals in Group 13 in the Periodic Table, such as aluminium and indium, it has been reported in literature that metal carboxylates can be synthesized by reacting metal hydroxides with carboxylic acids.[64-66] For instance, indium (III) formate and indium (III) acetate, can be made by reacting indium (III) hydroxide with formic acid and acetate acid, respectively. Figure 2.3 illustrates a hypothetical scheme for the removal of $In(OH)_3$ from an ITO surface using ferrocene carboxylic acid (FcCA) modifier. It is assumed that an $In(OH)_3$-FcCA complex is formed via a condensation reaction, and the complex is assumed to be soluble in the solvent used for FcCA adsorption (ethanol). When indium hydroxide species are removed from the surface, more electroactive sites on ITO surface are

available for the charge transfer of free redox molecules in solution. Since the other modifiers also have acidic groups, the complex formation via condensation reaction is assumed to be possible between $In(OH)_3$ and the other modifiers.

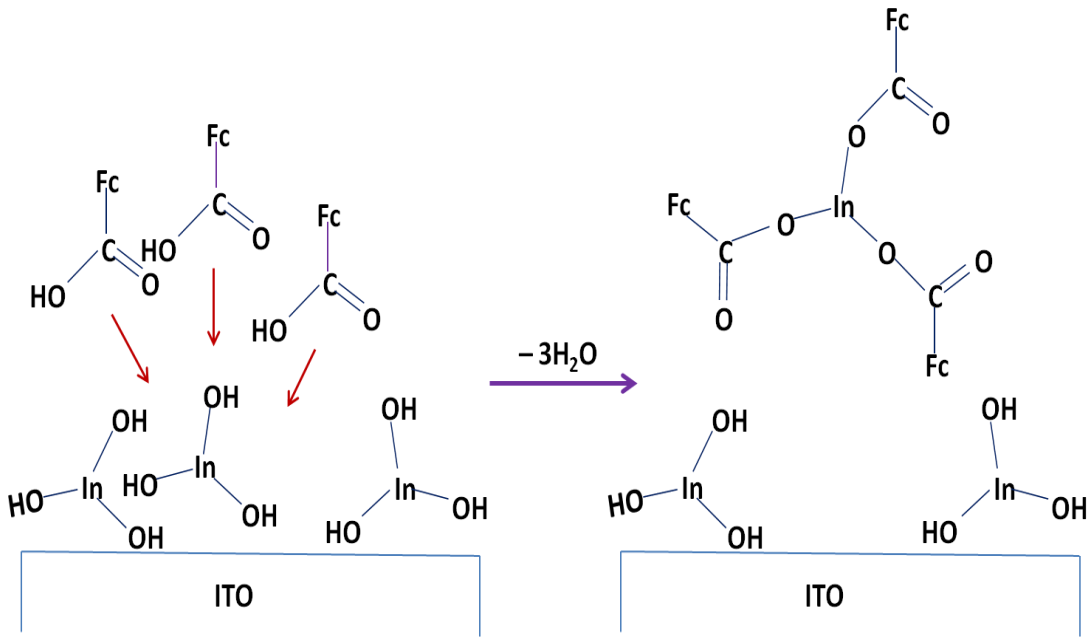

Figure 2.3 Proposed scheme for the removal of $In(OH)_3$ from an ITO surface via $In(OH)_3$-FcCA complexation.

Carter et al. compared k° before and after modification of ITO using carboxylic acid containing modifiers, and they observed the enhancement of k° after the modification for both ferrocene and TPD (N,N,N′,N′-

tetraphenyl-biphenyl-4,4′-diamine) redox probes.[22] Moreover, they observed that a carboxylic acid terminated gold electrode captured indium (In) from an EtOH solution containing In_2O_3 powder.[22] Since In_2O_3 powder and ITO showed comparable degrees of hydroxylation in an ambient environment, the powder was used as a high surface area analogue of ITO.[3, 22] The detection of In was suggested as an indication of indium hydroxide species removal on ITO by carboxylic acid containing modifiers.[22]

In this study, modifiers with different acidic groups (Figure 1.2) were studied to evaluate the impact of binding group on the charge transfer reaction at the surface of ITO. Firstly, redox potentials and charge transfer rates of dissolved modifiers were investigated before binding to ITO surface. Secondly, evaluation of adsorbed layers of the modifiers was performed to investigate adsorption coverages, redox potentials, and charge transfer rates of the different modifiers when tethered to ITO. Finally, the impact of the surface modifications was investigated by evaluating the change in the charge transfer rates of a solution redox probe.

2.2 Experimental

The ITO-coated planar electrodes used in this study were purchased from Colorado Concept Coatings LLC (model S1X0015), with a coating thickness of 1200 – 1600 Å and sheet resistance of 9 – 15 Ω/sq. Commercially available ferrocene (Fluka), ferroceneacetic acid (FcAA, Aldrich), ferroceneboronic acid (FcBA, Aldrich), and ferrocenecarboxylic acid (FcCA, ScienceLab) were used as well as the molecules synthesized by O'Neil Smith in Department of Chemistry and Biochemistry at Georgia Institute of Technology, ferrocenehydroxamic acid (FcHA), ferrocenephosphonic acid (FcPA), and ferrocenesulfonic acid (FcSA). A teflon electrochemical cell (electrode area: 0.673 cm^2) was used for cyclic voltammetry (CV) experiments. All electrochemical measurements were performed on a CH Instruments Electrochemical Workstation (CHI420A). The second scan of the CV was used for all reported values and calculations unless otherwise noted. A 0.1 M tetrabutylammonium perchlorate (TBAP, Aldrich) in ethanol (EtOH, Decon) or acetonitrile (ACN, EMD) was used as supporting electrolyte. A Basi Non-Aqueous Reference Electrode kit was used for all experiments. A 0.01 M silver nitrate ($AgNO_3$) in the 0.1 M TBAP solution was used as the filling solution for the $Ag/AgNO_3$ reference

electrode. The potential of the reference electrode is 0.351 V vs. a normal hydrogen electrode (NHE).[67]

2.2.1 Dissolved molecule experiments

ITO slides were cleaned as described in Section 2.2.2.1 before taking measurements. Each molecule was dissolved in 0.1 M TBAP/EtOH to achieve a 1 mM solution. The reference electrode filling solution was 0.01 M $AgNO_3$ in 0.1 M TBAP/EtOH. Scan rates of CV experiments were 0.1, 0.5, or 1 V/sec. A potential range for scanning was chosen to be wide enough to determine the peak potential at the highest scan rate. The potential windows were -0.7 – 0.7 V, -0.6 – 0.4 V, -0.5 – 0.5 V, -0.25 – 0.55 V, -0.25 – 0.7 V, -0.5 – 0.5 V, and -0.5 – 0.5 V for Fc, FcAA, FcBA, FcCA, FcHA, FcPA, and FcSA respectively.

2.2.2 Adsorbed layer experiments

All CV experiments for adsorbed layers were done with a scan rate of 0.1 V/sec. The electrolyte solution was 0.1 M TBAP/ACN and the reference electrode filling solution was 0.01 M $AgNO_3$ in 0.1 M TBAP/ACN. A potential range for scanning was chosen to be wide enough to determine the

starting and ending point of peaks. The potential windows were -0.4 – 0.6 V, -0.2 – 0.7 V, -0.2 – 0.6 V, -0.5 – 0.5 V, and -0.3 – 0.8 V for FcAA, FcCA, FcHA, FcPA, and FcSA respectively.

2.2.2.1 Cleaning of ITO slides

ITO slides were cleaned by gentle rubbing with nitrile gloves with 1% Triton X-100 solution for 1 min, then sonicating for 10 min each in 1% Triton X-100, nanopure water, and ethanol. After ethanol sonication, the slides were dried with nitrogen flow. Lastly, air plasma (Harrick model PDC-3XG) cleaning/activating was conducted for 10 min at 30 W.

2.2.2.2 Adsorbed layer formation

The 1 mM solutions of each adsorbate were used to find the steady state surface coverage as a function of adsorption time. The solvents used in the adsorption process were ethanol (for FcAA, FcCA, and FcPA), chloroform (for FcSA), THF (for FcHA), and toluene (for FcBA). Cleaned ITO slides were soaked in each solution (40 mL), contained in a glass Coplin staining jar, for a range of time from 1 min to 48 hr (and up to 98 hr for FcAA).

The concentration of the adsorbed layer formation solution was varied with constant adsorption time (24 hr) for the adsorption isotherm experiments. The range of concentrations was 1 µM – 3 mM, 10 µM – 5 mM, 0.1 µM – 2 mM, 0.1 µM – 5 mM, and 50 µM – 2.5 mM for FcAA, FcCA, FcHA, FcPA, and FcSA respectively. Cleaned ITO slides were soaked in each solution (~ 20 mL), contained in a 20 mL beaker, covered with parafilm or aluminum foil, for 24 hr. All adsorbed layer formations were done at room temperature (~ 25 °C).

2.2.2.3 Post-treatment

ITO slides were removed from the adsorbed layer formation solution after specified adsorption times and rinsed with the pure solvent that was used in the adsorption step. After the rinse, sonication was done in the pure solvent for 5 min to remove physisorbed molecules or contaminants.

2.2.3 Solution probe experiments

Solution probe (Fc) was dissolved in 0.1 M TBAP/ACN to prepare 1 mM solution. The reference electrode filling solution was 0.01 M $AgNO_3$ in

0.1 M TBAP/ACN. CV experiments were performed for modified (24 hr adsorption of each modifier) and unmodified ITO electrodes with the presence of Fc in solution. Scan rates of CV experiments were 0.1, 0.5, or 1 V/sec. A potential range for scanning was chosen to be wide enough to determine the starting and ending point of peaks. The potential window was -0.25 – 0.45 V for all experiments.

2.3 Results and Discussion

2.3.1 Cyclic voltammetry of dissolved molecules

Example cyclic voltammograms for dissolved molecule experiments are presented in Figure 2.4. The time elapsed between injection of the molecule into the cell and acquisition of the CV was relatively short (< 10 min). The peak currents of adsorbed layers formed during 10 min adsorption time are small (typically less than 2%) compared to the peak currents of dissolved molecule experiments. Based on this result, the current response shown in Figure 2.4 can be regarded as mainly representing the diffusion controlled charge transfer reaction.

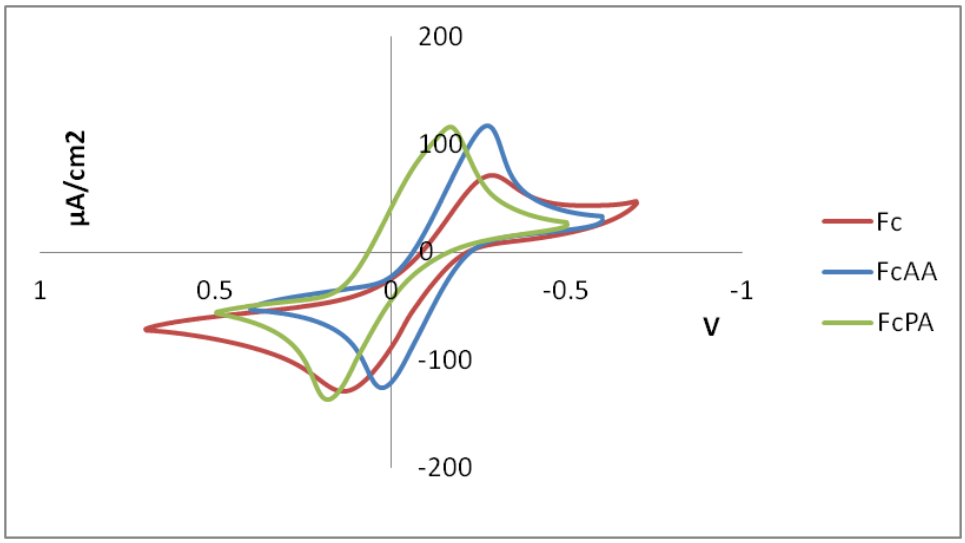

Figure 2.4 Cyclic voltammograms for 1 mM ferrocene, FcAA, and FcPA in 0.1 M TBAP/EtOH with 0.1 V/s scan rate.

A redox potential was determined as the half-peak potential ($E_{1/2}$), which is the midpoint between the oxidation peak potential and the reduction peak potential. For determination of the charge transfer rate constant (k°) for each molecule, cyclic voltammetry experiments of dissolved ferrocene and substituted ferrocenes at different scan rates (0.1, 0.5, and 1 V/s) were conducted. Based on the peak separations, the charge transfer rate constant (k°) for each molecule was calculated using "Nicholson's method" as described in Appendix A. The determined values are summarized in Table 2.1.

Table 2.1 Summary of redox potentials of ferrocene and substituted ferrocenes, Hammett constants for the acid substituents, and the charge transfer rate constants of the ferrocene derivatives.

	Fc	FcAA	FcBA	FcCA	FcHA	FcPA	FcSA
$E_{1/2}$ (V)	-0.073 ± 0.007	-0.117 ± 0.006	-0.060 ± 0.002	0.136 ± 0.007	0.17 ± 0.01	0.008 ±0.003	-0.018 ± 0.002
σ_p	0	-0.07[a]	0.12[b]	0.45[b]	N/A	0.42[b]	0.64[c]
$10^4 k°$ (cm/s)	6.7 ± 0.3	9.7 ± 0.8	8.6 ± 0.8	13 ± 1	10 ± 1	7.9 ± 0.1	8.9 ± 0.2

[a] Landy, D.; Fourmentin, S.; Salome, M.; Surpateanu, G. *J. Incl. Phenom. Macrocycl. Chem.* **2000,** *38*, 187. [b] Hansch, C.; Leo, A.; Taft, R. W. *Chem. Rev.* **1991,** *91*, 165. [C] Imaizumi, H.; Koyanagi, T.; Zhao, D. *J. Radioanal. Nucl. Chem.* **2002,** *252*, 467.

2.3.1.1 Redox potentials of dissolved molecules

The Hammett constant (σ_p) for a given substituent is defined as log Z - log Z°, where Z is the ionization constant for a substituted benzoic acid in water at 25 °C, and Z° is the ionization constant for benzoic acid itself.[68] Thus, the Hammett constant represents the electron donating/withdrawing property of a substituent. Linear relationships between the redox potentials of ferrocene derivatives and the Hammett constants of the substituents have been reported in literature.[69-71] Due to the electron donating/withdrawing

property of the substituent, the redox potential of the substituted ferrocenes examined here were expected to be shifted from the redox potential of ferrocene. Based on the Hammett constant of each substituent, AA is the only electron donating substituent, so it is expected that FcAA would be more readily oxidized than ferrocene. The redox potential ($E_{1/2}$) of FcAA from the measurement was less positive than that of ferrocene, which agrees with the prediction (Table 2.1). However, the linearity expected between the Hammett constant and the redox potential was poor as shown in Figure 2.5 (a), and greatly improved when FcCA and FcSA are omitted from the graph (Figure 2.5 (b)).

Emilia et al. reported that FcCA in tetrahydrofuran (THF) deviated from the linear trend of σ_p vs. $E_{1/2}$ constructed from many other substituted ferrocenes, whereas it followed a linear trend in dichloromethane (DCM) or in ACN-$MClO_4$ (M = Li or Na).[69] Even though they did not mention what property of the solvents was responsible for the differences, it can be assumed that the solvent used for measurements is the factor that determines whether a molecule follows the linear behavior or not. Thus, the solvent used in this experiment, ethanol (EtOH), was assumed to cause the non-linear behavior of FcCA and FcSA. Roberts and Silver studied the molecular

orbital energy levels of ferrocene derivatives using Mössbauer spectroscopy (gamma ray spectroscopy).[72] They reported a linear relationship between the Mössbauer parameters and the Hammett constants of ferrocene derivatives but a non-linear behavior for FcCA. Since the spectra were measured using the solids of the ferrocene derivatives while the Hammett constants were measured using the solutions, they assumed that the non-linearity of FcCA was produced because hydrogen bonding between molecules in solid phase is different from that in solution phase. However, this does not explain the solvent dependent behavior of FcCA, and a molecular level explanation of the solvent effect has not been found yet. To verify the assumption that the solvent determines whether a molecule follows the linear behavior or not, additional experiments with other solvents, in which all the modifiers can be dissolved, would be necessary.

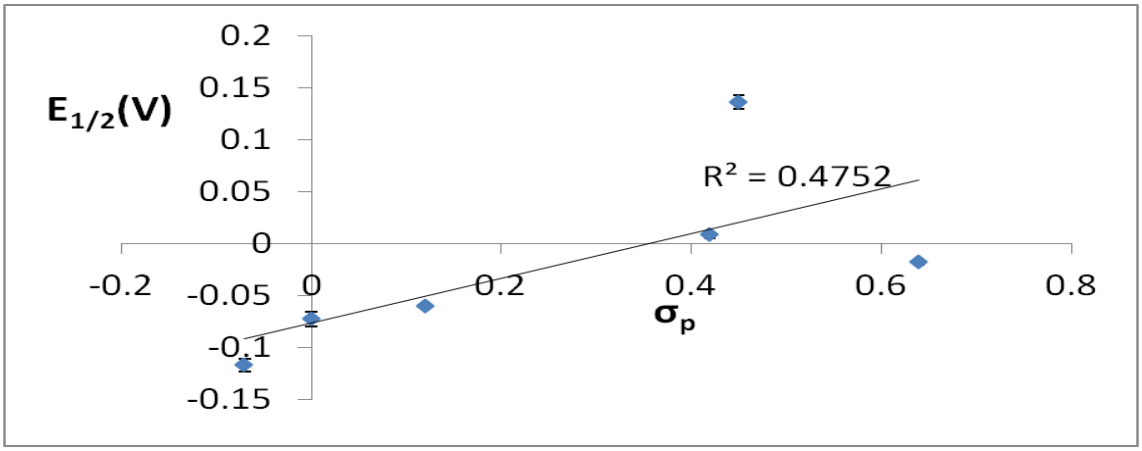

(a)

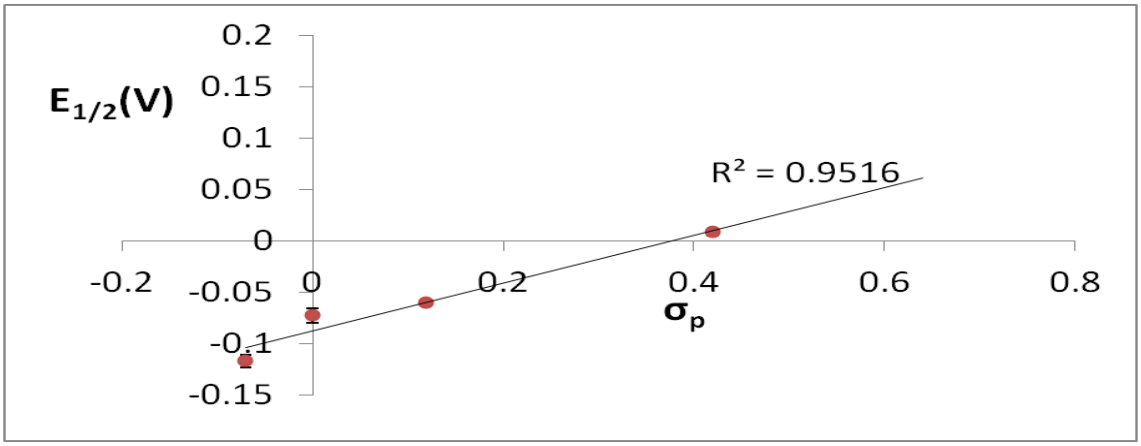

(b)

Figure 2.5 Redox potential ($E_{1/2}$) versus Hammett constant (σ_p) plots. Values of all modifiers are included in (a), and FcCA and FcSA are omitted in (b).

2.3.1.2 Charge transfer rate constant of dissolved molecules

According to the expression for the charge transfer constant (k°) described by Nicholson (Equation A.1 in APPENDIX A), k° is directly proportional to $\left\{\frac{D_O}{(D_O/D_R)^{\alpha}}\right\}^{1/2}$, where D_O and D_R are the diffusion coefficients of oxidized and reduced forms of an electroactive species, and α is the transfer coefficient. Based on the Stokes-Einstein relation, the diffusion coefficients of different molecules in the same solvent are mainly dependent on the size of the molecule.[73, 74] Since the sizes of the substituted Fcs do not vary significantly from Fc (within a few Å), the diffusion coefficients of substituted Fcs were assumed to be the same as the diffusion coefficient of Fc in ethanol, 1×10^{-5} cm^2/s.[75] Additionally, $D_O = D_R$ was assumed since the difference between oxidized and reduced forms of the molecules is only one electron loss or gain. Based on these factors, k° of Fc and substituted Fcs were expected to be close. However, as shown in Table 2.1, the values of k° for substituted Fcs are generally higher than Fc.

When the assumptions and the expectations mentioned above are kept, $k°_0$ in Equation 2.1 for Fc and substituted Fcs are assumed to be close. A possible explanation for the difference in k° is a difference in θ, the fractional area of the electroinactive region. As described in Section 2.1.2,

Carter et al. suggested that the electroinactive indium hydroxide species on the surface of ITO could be removed by carboxylic acid containing modifiers.[22] The value of θ can be reduced when the electroinactive indium hydroxide species is removed from the surface, which leads to an enhancement of k°. Since the k° of all the substituted Fcs are higher than the k° of Fc, the removal indium hydroxide species (electroactivation) is assumed to be occurred with every modifier. The relatively higher value of k° for FcCA compared to other modifiers suggests that FcCA can remove more indium hydroxide species from the surface during the elapsed time of the experiment (< 10 min). Interpretation of the slightly lower value of k° for FcPA is a little more complicated. Charge transfer coefficients (α) of all molecules were assumed as 0.5. However, the reduction peak of FcPA is broader than the oxidation peak (Figure 2.4), which may suggest that α of FcPA is lower than 0.5 while the symmetrical shapes of the oxidation and reduction peaks for the other molecules suggest α is close to 0.5. In Nicholson method, as the peak separation becomes wider, the impact of α on the peak separation becomes greater. Since ψ is calculated based on the peak separation, the deviation of calculated ψ (assuming $\alpha = 0.5$) from the "true" ψ (using the actual α) will also be greater for the wider peak separation.

Thus, the linearity of the ψ vs. $\nu^{-0.5}$ plot (see Appendix A) will be reduced when the impact of α is increased. However, as shown in Figure A.3 (Appendix A), the linearity of the ψ vs. $\nu^{-0.5}$ plot for FcPA is comparable to those for other molecules, which suggests that the impact of α is not noticeable. Because α most likely does not play a role, the slightly lower value of k° for FcPA is assumed to be the result of less electroactivation of the surface.

2.3.2 Adsorbed layers

2.3.2.1 Binding mechanism of tethered ferrocene

Ferrocene molecules with different substituents were deposited onto ITO substrates via adsorption from solution. Possible mechanisms of binding between substituents and a metal oxide surface are a heterocondensation reaction that involves coordination binding or a reaction that occurs without coordination as shown in Figure 2.6. For highly Lewis acidic sites such as surface exposed metals, coordination can occur through the double bonded oxygen in the substituents.[76-80] If the surface is fully hydroxylated, heterocondensation can occur without the coordination.[81] Hydrogen bonding can occur instead of heterocondensation during the

adsorption process, so the binding mode can be varied from monodentate to multidentate.[80] Because the other acidic functional groups used in this study also contain double bonded oxygen atoms or hydroxyl groups, the binding mechanism of phosphonic acid is assumed to be valid for the other acidic functional groups as well.

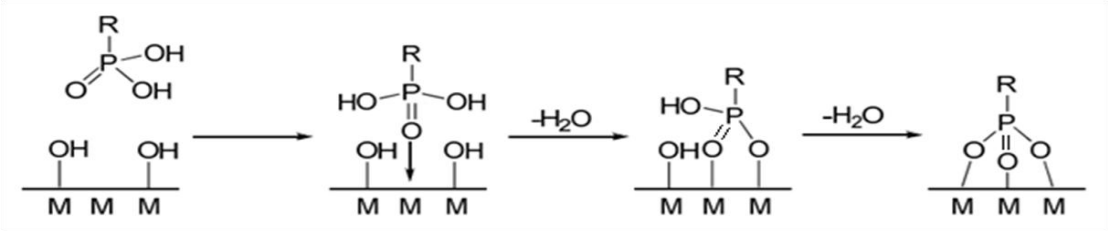

(a)

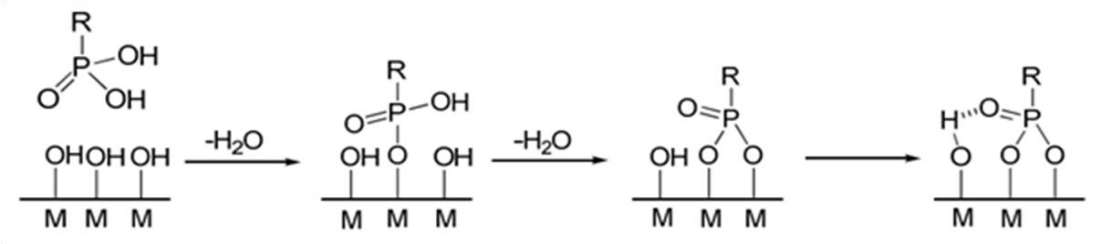

(b)

Figure 2.6 Binding schemes of phosphonic acids on metal oxide surfaces. Processes either begin with coordination bonding (a) or without it (b).[4] (Adapted from Ref. 4).

2.3.2.2 Electroactive surface coverage of tethered ferrocene films

In order to determine a standard condition for the electroactive surface coverage comparison among different modifiers, the electroactive surface coverage of each modifier was measured at different adsorption times (30 sec – 48 hours). The measured electroactive surface coverages were varied with the adsorption time as shown in Figure 2.7. As the adsorption time increased, the electroactive surface coverage increased and reached a steady state. Since the steady state electroactive surface coverages were observed within 24 hours for all modifiers except FcAA, the electroactive surface coverages from 24 hour adsorptions were selected for comparison.

Extended adsorption times for FcAA were investigated since it was difficult to observe a trend in the electroactive surface coverage within 48 hours. When the time was extended to 98 hours, the steady state electroactive surface coverage of FcAA was observable after 60 hours. In Section 2.3.2.4, a significant enhancement in the charge transfer rate of FcAA was observed from 24 hour adsorption compared to 30 min adsorption, and aggregation of FcAA was hypothesized to explain the enhancement. If the hypothesis is valid, it may be related to the relatively long time required for FcAA to reach the steady state electroactive surface coverage.

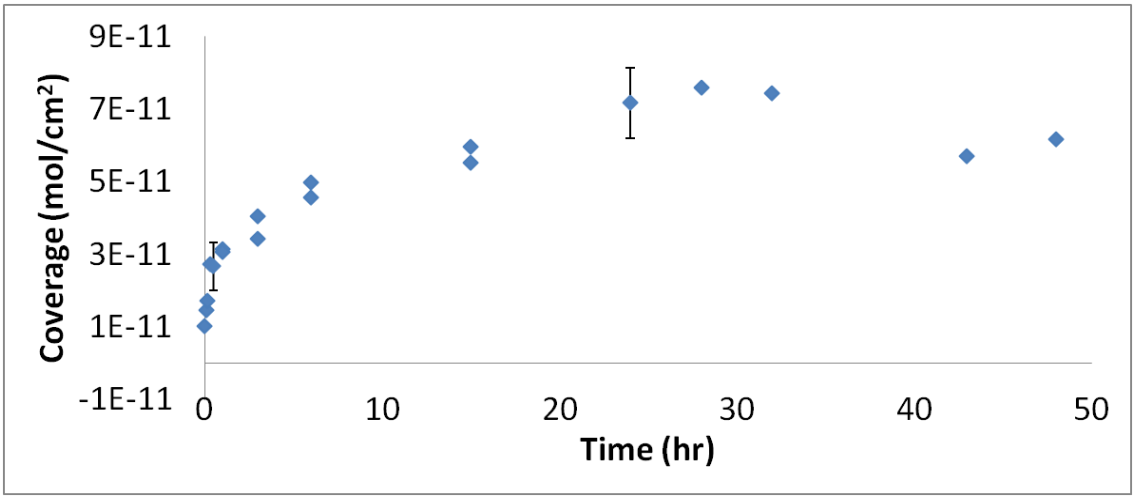

(a)

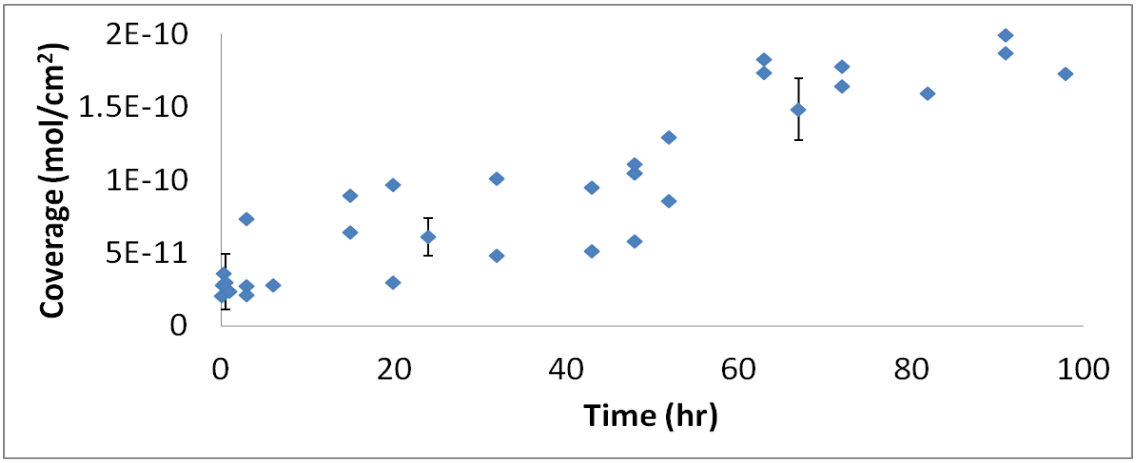

(b)

Figure 2.7 Time dependent electroactive surface coverage for FcCA (a) and FcAA (b).

As shown in Table 2.2, the electroactive surface coverages measured from 24 hour adsorptions of different modifiers varied. Binding constants

and theoretical surface coverages of close-packed monolayers are also listed in Table 2.2 to investigate the impact of the binding affinity and the binding orientation on the electroactive surface coverage.

Table 2.2 Summary of electroactive surface coverage, theoretical surface coverage of close-packed monolayers, projection area range, and binding constant of each modifier.

	FcAA	FcCA	FcHA	FcPA	FcSA
$10^{10}\Gamma$ (mol/cm^2) from CV	0.6 ± 0.1	0.7 ± 0.1	1.05 ± 0.07	2.9 ± 0.3	1.1 ± 0.4
$10^{10}\Gamma$ range (mol/cm^2) from modeling	3.6 – 6.8	5.1 – 8.8	4.0 – 8.3	3.6 – 6.9	3.4 – 6.6
Projection area range (Å^2/molecule)	24 – 46	19 – 33	20 – 41	24 – 47	25 – 48
Binding constant (M^{-1})	$(1.4 \pm 0.8) \times 10^3$	$(3.8 \pm 0.7) \times 10^3$	$(1.1 \pm 0.3) \times 10^6$	$(2.8 \pm 0.5) \times 10^6$	$(8 \pm 4) \times 10^2$

It was expected that a molecule with a relatively high probability of binding would have a relatively large surface coverage. Thus, the binding affinity of each modifier was considered as a source of the variation in the electroactive surface coverages among the different modifiers. In order to quantitatively evaluate the binding affinities of modifiers, the binding constant of each modifier was calculated. This was achieved by fitting the

electroactive surface coverage vs. concentration plot with the Langmuir isotherm model, as shown in Figure 2.8. Using the Langmuir isotherm, a binding constant, K_a, can be described with the following equation.[82-84]

$$K_a = \frac{\vartheta}{[M](1-\vartheta)} \qquad (2.2)$$

where [M] is the concentration of a modifier in solution, and ϑ is the fractional electroactive surface coverage (i.e. Γ / Γ_{max}, Γ_{max} is obtained from the fitting curve). Several orders of magnitude difference in the binding constants (Table 2.2) suggests that the binding affinity of each modifier to an electroactive site is noticeably different. Generally, binding constants for FcAA, FcCA, and FcSA, which showed relatively low electroactive surface coverages (ca. $\leq 1.1 \times 10^{-10}$ mol/cm^2), are on the order of 10^3 M^{-1}, whereas the binding constant for FcPA is on the order of 10^6 M^{-1}. The higher binding constant for FcPA coincides with the largest electroactive surface coverage observed with FcPA. However, even though the binding constant of FcHA is on the same order (10^6 M^{-1}) of magnitude as FcPA, its electroactive surface coverage is closer to the ones with low binding constants than to FcPA. Thus,

a conclusive statement regarding the relationship between the binding affinity and the electroactive surface coverage could not be derived.

Use of the Langmuir isotherm implies assumptions that all adsorption sites are equivalent and that one molecule is adsorbed to one site.[82, 83] Since the heterogeneity of the ITO surface and the possibility of multidentate binding of modifiers are not considered in the Langmuir isotherm, a more sophisticated isotherm expression may be necessary for more meticulous evaluation of the binding affinity.

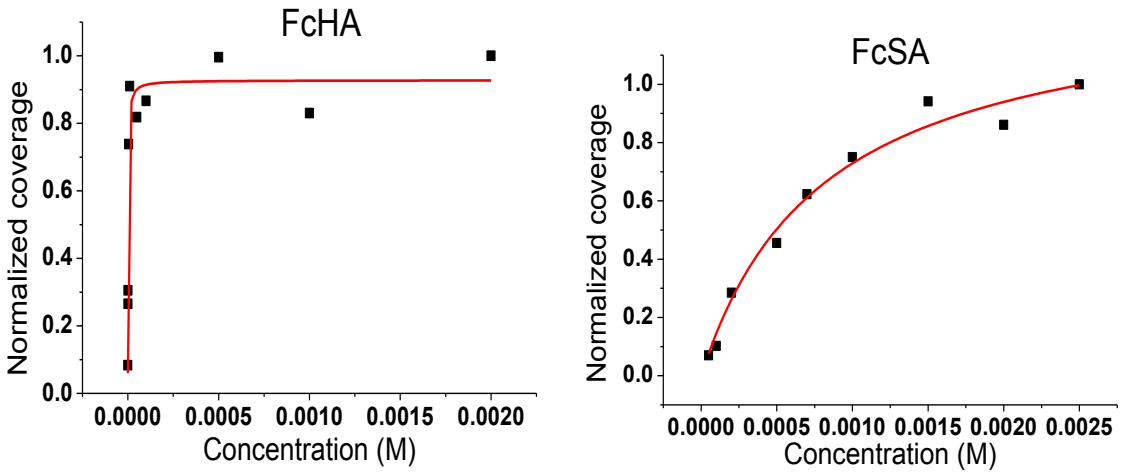

Figure 2.8 Adsorption isotherms of FcHA and FcSA adsorbed layers. The red lines are the theoretical fit to the Langmuir isotherm.

The effect of the binding orientation on the surface coverage was evaluated using a modeling program. Possible binding orientations were visualized by Spartan modeling software as shown in Figure 2.9, and the rectangular projection area per molecule for each orientation was calculated. Based on the calculated maximum and minimum projection areas, the surface coverage range of a close-packed monolayer for each molecule was determined.

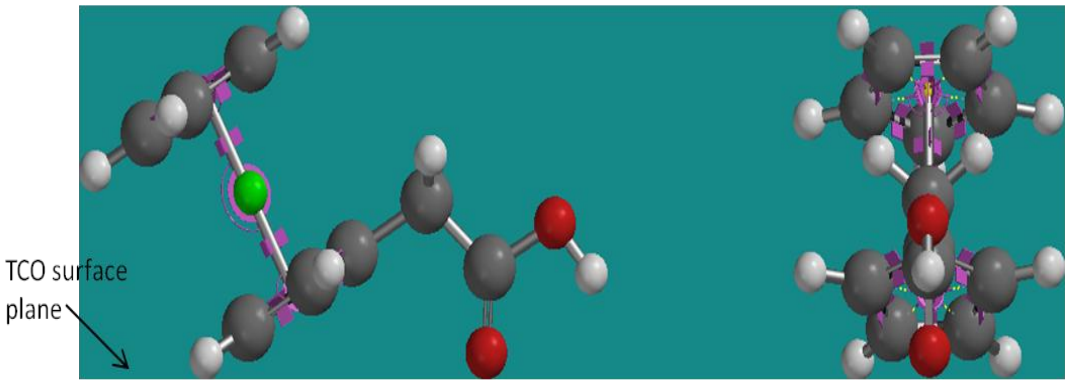

(a)

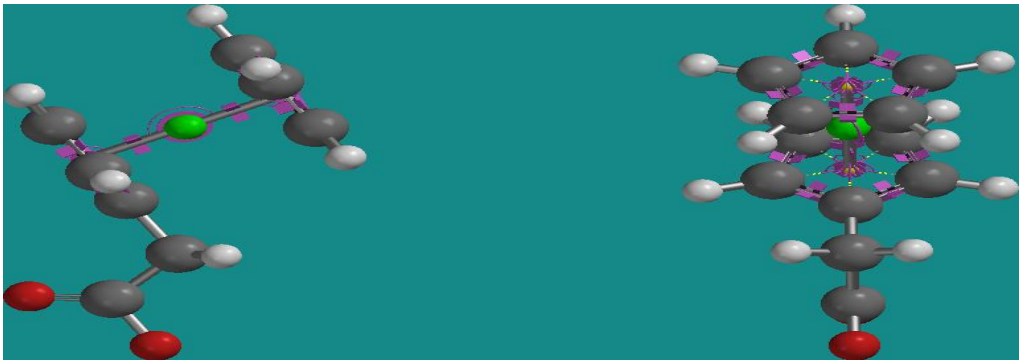

(b)

Figure 2.9 Possible binding orientations of FcAA on an adsorbent surface for maximum projection area (a) and minimum projection area (b). Side views (left) and front views (right).

The ranges of the close-packed monolayer surface coverages listed in Table 2.2 show that binding orientation can vary the coverage up to approximately a factor of two. The effect of the binding orientation can also

be applied to the variation in the electroactive surface coverage since the number of molecules bound to the electroactive region is also limited by the area taken by individual molecules. However, the result also suggests that the binding orientation is not the only factor that controls the electroactive surface coverage. For instance, the electroactive surface coverage measured for FcPA is ca. 3 – 5 times larger than the electroactive surface coverage of other modifiers. The difference cannot be explained solely by the binding orientation even if the smallest projection area for FcPA and the largest projection area for other modifiers are selected. More information on binding orientation is expected to be achieved in the future by analyzing the adsorbed layer using a spectroscopic technique such as photoelastic modulation infrared reflection absorption spectroscopy (PM-IRRAS).

The electroactivation of the surface by modifiers was also considered as a possible factor that affects the electroactive surface coverage. If the degree of the electroactivation for each modifier is different and all electroactivated sites are occupied by modifiers, then the electroactivation can be a limiting factor for the electroactive surface coverage variation among different modifiers. Based on the results of the dissolved molecule experiments discussed in Section 2.3.1.2, FcCA was expected to have a

relatively higher degree of electroactivation than other modifiers, and FcPA was expected to have a relatively lower degree of electroactivation than other modifiers. However, neither the electroactive surface of FcCA was the largest nor the electroactive surface of FcCA was the smallest (Table 2.2). Nevertheless, the degree of the electroactivation by individual modifiers at 24 hour adsorption may not be the same as that within 10 minutes (elapsed time for dissolved molecule experiments). In Section 2.3.3, the electroactivation by the modifiers at 24 hour adsorptions was discussed with respect to the variation of the charge transfer rate of the solution probe. However, since the electrocatalytic effect can concurrently be involved in the variation of the charge transfer rate, a discrete evaluation of the electroactivation effect could not be assessed. Thus, a conclusive statement on the relationship between the electroactivation and the electroactive surface coverage has not been made. The experiment that may allow a further discussion on the relationship between the electroactivation and the electroactive surface coverage is described in Section 2.3.3.

The electroactive surface coverage of adsorbed layers decreased as more sequential scanning was conducted. Figure 2.10 shows the percent loss of the coverage at the 10^{th} scan compared to the initial scan. The diagram

shows that the FcPA adsorbed on the ITO surface is more electrically stable than the other modifiers. The difference in the stability of the modifiers is assumed to be related to the binding mode. As mentioned in Section 2.3.2.1, binding modes of a modifier may vary from monodentate to multidentate. Since multiple bonds will likely immobilize a modifier more tightly onto the surface (i.e. require more energy to be broken and mobilize the modifier) than a single bond, an adsorbed modifier with multidentate binding will be more stable. It is hard to predict what binding mode will be predominant for each modifier from previous studies because different binding modes were reported even for the same binding group on different metal oxides.[85] However, there is a paper that reported the major binding mode of phosphonic acid adsorption to ITO surface.[86] Using PM-IRRAS analysis, bidentate binding was suggested as the major binding mode of phosphonic acid adsorption to ITO, in which P=O is left unattached. The free P=O moieties suggest that the binding mechanism of phosphonic acid is mainly heterocondensation without coordination as described in Figure 2.6 (b). Thus, it is assumed that the number of hydroxyls in the binding group determines the main binding mode. Among the acidic groups used in the adsorbed layer study, only phosphonic acid has two hydroxyls while the others have one.

From this, it is predicted that FcPA adsorbs mainly using the bidentate mode while monodentate is the main binding mode for the others. The stability of each modifier illustrated in Figure 2.10 agrees with the prediction that FcPA is noticeably more stable than other modifiers.

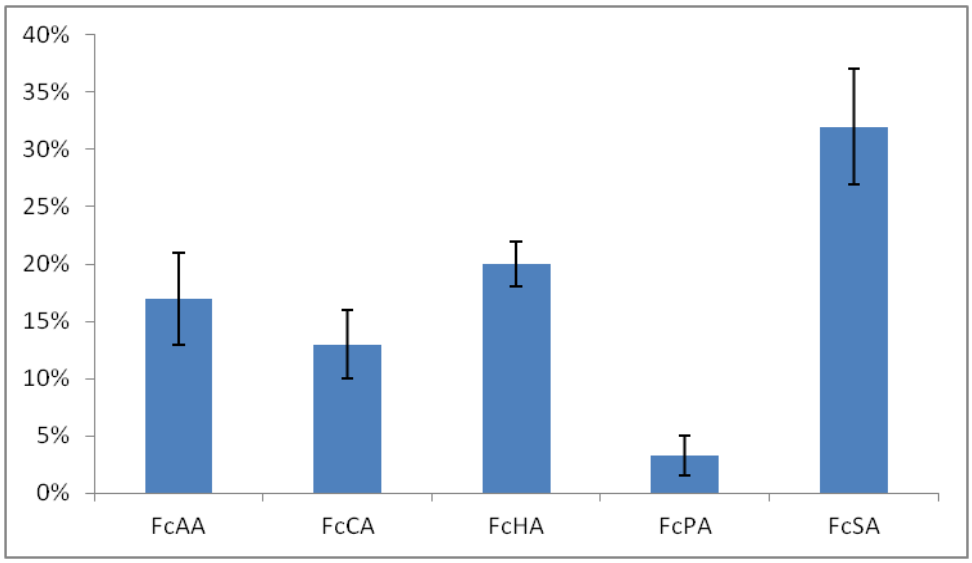

Figure 2.10 Surface coverage loss at 10th scan of CV for adsorbed layers on ITO prepared from 24 hour adsorption.

2.3.2.3 Redox potential of adsorbed layers

Cyclic voltammetry experiments were performed after short time (30 min) adsorptions and long time (24 hr) adsorptions as shown in Figure 2.11

for FcCA and FcPA. The redox potentials of each adsorbed layer are summarized in Table 2.3.

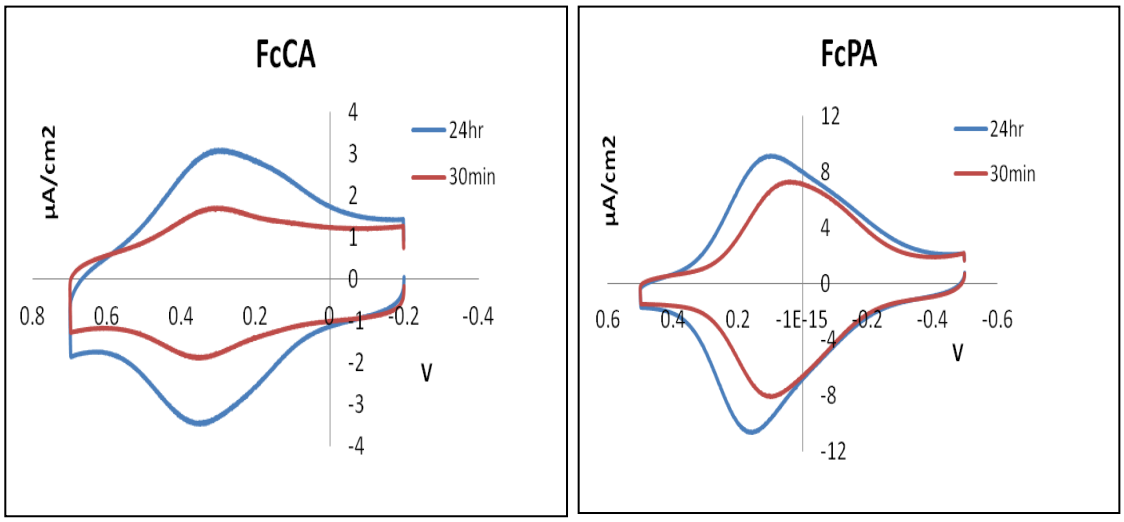

Firgure 2.11 Cyclic voltammograms of FcCA and FcPA adsorbed layers at 30 min soaking vs. 24 hour soaking.

Table 2.3 Redox potentials ($E_{1/2}$) of the adsorbed layers with short time (30 min) adsorption vs. long time (24 hour) adsorption.

Time		FcAA	FcCA	FcHA	FcPA	FcSA
30 min	$E_{1/2}$ (V)	0.00 ± 0.04	0.33 ± 0.01	0.22 ± 0.01	0.05 ± 0.02	0.37 ± 0.01
24 hr		0.09 ± 0.01	0.32 ± 0.01	0.27 ± 0.01	0.11 ± 0.02	0.31 ± 0.02

The relationship between the redox potentials and the Hammett constants was investigated as had been done for the dissolved molecule experiments discussed in Section 2.3.1.1. For adsorbed layers, the inclusion of FcPA caused poor linearity of $E_{1/2}$ vs. σ_p plot as shown in Figure 2.12 (a). However, the molecules that caused the poor linearity of the dissolved molecule experiments, FcCA and FcSA, showed a good linear trend in this case when FcPA was omitted (Figure 2.12 (b)). As discussed in Section 2.3.1.1, the solvent used for measurements was assumed to be an important factor that determines whether a molecule shows linear or non-linear behavior in the $E_{1/2}$ vs. σ_p plot. The assumption is supported by the above result that the linear trend was observed for FcCA and FcSA when they were measured with acetonitrile (ACN), but not with ethanol (EtOH). Additionally, the linear behavior of FcCA with ACN in this experiment agrees with the observation from Emilia et al. that FcCA followed the linear trend with ACN-based solvents (ACN-$LiClO_4$ or ACN- $NaClO_4$).[69] The linear behavior of dissolved FcPA and the non-linear behavior of adsorbed FcPA may also be due to the change of the solvent used for measurements.

The interaction between FcPA and ITO may be another factor that is responsible for the non-linear behavior of the adsorbed FcPA in the $E_{1/2}$ vs.

σ_p plot. As shown in Figure 2.10, FcPA adsorbed on ITO is more stable than the other modifiers, and the multidentate binding of FcPA was assumed to be a cause of the stability in Section 2.3.2.2. From this, the interaction between FcPA and ITO is assumed to be stronger than the interactions between the other modifiers and ITO. If the interaction between a modifier and ITO can change the electron donating/withdrawing property of the acidic functional group (substituent), the change would likely be more significant for FcPA than the other modifiers, and hence the behavior of FcPA in the σ_p vs. $E_{1/2}$ plot could deviate from that of the other modifiers.

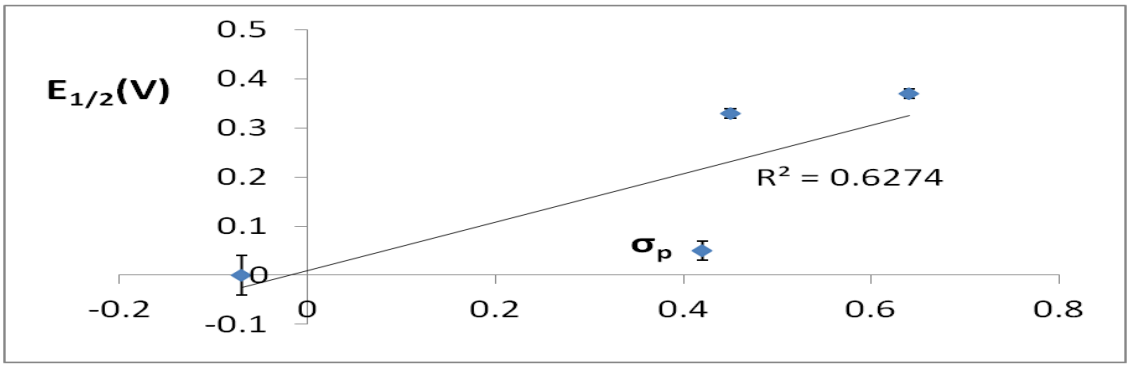

(a)

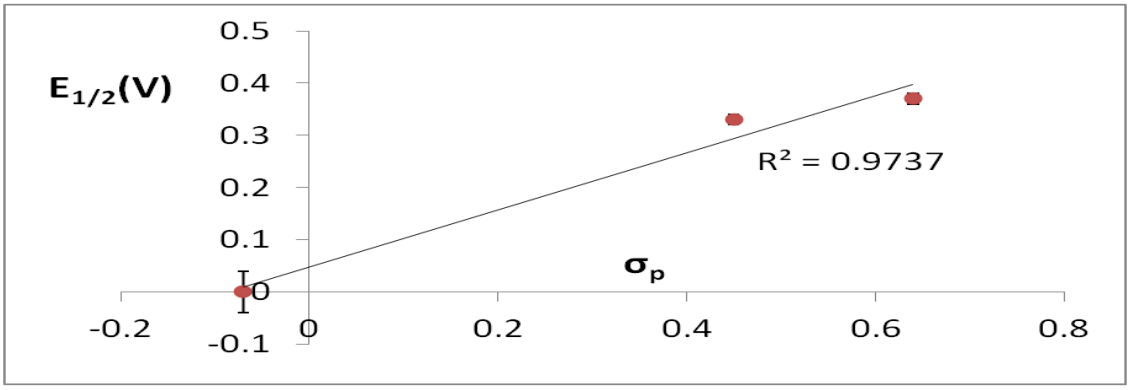

(b)

Figure 2.12 Redox potential ($E_{1/2}$) versus Hammett constant (σ_p) plots for 30 min adsorptions. Values of FcAA, FcCA, FcPA, and FcSA are included in (a), and FcPA is omitted in (b).

As the adsorption time increased, the redox potentials of the adsorbed layers were shifted except for the FcCA layer (Table 2.3). Positive shifts were observed for FcAA, FcHA, and FcPA, and a negative shift was

observed for FcSA. The redox potential of FcCA did not show any statistical difference between 30 min and 24 hour adsorptions. The linearity of the the σ_p vs. $E_{1/2}$ plot was somewhat altered by the redox potential shifts. The coefficient of determination (R^2) of linear fitting curves for 24 hour adsorptions were 0.5455 and 0.9127 for FcPA included plot and FcPA omitted plot respectively, which are lower than those for 30 min adsorptions.

According to theory, the peak width at half-height of a cyclic voltammogram of one electron transfer reaction is expected to be 90.6 mV for an adsorbed redox active species.[52] However, the peak width at half-height observed from the voltammograms of adsorbed layers (Figure 2.11) were relatively broad (> 200 mV) for all the modifiers in both 30 min and 24 hour adsorptions, from which it is assumed that the peaks are composed of more than one constituent. Since their redox potentials are close enough to form one broad peak instead of discrete peaks, and the modifier was the only electroactive species present, the constituents are expected to be the results of the variation in the binding modes and/or the results of the different binding locations that may have different charge densities.

A binding mode distribution can be responsible for the multiple components of the peak in the voltammogram. Even though predominant

binding modes were suggested in the previous section, minor binding modes can coexist. For instance, Weng et al. determined the composition of the binding modes of carboxylic acid onto TiO_2 as 63% monodentate, 34% bidentate, and 3% ionic or hydrogen bondings.[87] Additionally, using density functional theory (DFT) calculations, Li et al. suggested that the binding modes of phosphonic acids on some adsorption sites of ITO can be changed as a function of the surface coverage.[88]

Commercially available ITOs typically consist of crystalline grains that have a random distribution of exposed <100> and <111> planes of the In_2O_3 bixebyte lattice.[3, 21, 89, 90] If the charge density in different regions of ITO varies, the local potential can be different, and hence the modifiers bound in different planes or grain boundaries can exhibit different redox potentials. The multiple redox potentials can be responsible for the multiple components of the peak in the voltammogram.

The surfaces of crystalline materials are commonly composed of steps and terraces.[91] Ji et al. reported that the local potentials at steps and terraces varied when voltage was applied to the surface of graphene.[92] However, the difference in the local potential was ca. 1 mV when 1 V was applied to the

surface. Thus, the contribution of steps and terraces to the multiple components of the peak is not thought to be considerable.

The peak widths at half-height observed from 24 hour adsorptions (260 – 320 mV) were somewhat larger than those from 30 min adsorptions (240 – 300 mV). This suggests that the distribution of individual components is changed as the adsorption time increased. When the distribution is changed, the contribution from each component to the observed peak is changed. Thus, the change in the distribution is assumed to be a cause of the redox potential shifts of the modifiers with respect to the adsorption time.

Additionally, there is another effect that needs to be considered for redox potential variation as a function of time. The surface coverage of the adsorbed layer increases as the adsorption time increases. Consequently, the molecules are more densely packed as depicted in Figure 2.13, and it produces the higher degree of the intermolecular interaction between redox couples (ferrocenes). As a result, oxidation of ferrocenes becomes thermodynamically more difficult, and redox potential is expected to be shifted positively.

Figure 2.13 Illustration of the degree of the intermolecular interactions between redox couples, which depend on surface coverage.

The negative shift of FcSA and non-shift of FcCA, in which the positive shift expected from the intermolecular interactions was not observed, can be attributed to the change in the distribution of individual components at different times. However, the change in the distribution of individual components may also be contributed to the positive shifts of the other modifiers. Based on the CV data, it is difficult to determine which binding mode or region of ITO is responsible for a positive or negative redox potential relative to the others. If larger molecules (> 1 nm) that contain the same binding groups used in this study are available, the variation in the adsorption location as a function of the adsorption time could be studied using a high resolution surface imaging technique. Additionally, quantitative measurements of binding mode distribution at different adsorption times could be accomplished using a surface sensitive spectroscopic technique. The images and the measurements can be compared with the CV data, and

would likely provide more information about the relationship between molecule binding and redox potential.

2.3.2.4 Charge transfer rate constant of adsorbed layers

Using the cyclic voltammograms measured for short time (30 min) adsorptions and long time (24 hr) adsorptions, the charge transfer rate constants (k_s) were calculated for the adsorbed layers using the Laviron method that is described in Appendix B. The results are listed in Table 2.4.

Table 2.4 Charge transfer rate constants for adsorbed layers with short time (30 min) adsorption vs. long time (24 hr) adsorption.

Time		FcAA	FcCA	FcHA	FcPA	FcSA
30min	Charge transfer rate (s^{-1})	3 ± 1	4.6 ± 0.9	2.1 ± 0.3	2.2 ± 0.2	1.2 ± 0.3
24hr		10 ± 4	3 ± 1	3.6 ± 0.6	2.0 ± 0.2	0.96 ± 0.03

The charge transfer rate of adsorbed layers seems to be independent of the time of adsorption except in the case of FcAA. The independence of k_s from the time of adsorption suggests that k_s is not correlated to the redox potential shifts discussed in the previous section. In other words, the

distribution in bindings (binding location or binding mode) can vary the redox potential of a modifier, but the distribution does not alter the charge transfer rate measured for the modifier because either it had no effect on the charge transfer rate or the effect of each component in the distribution is averaged.

A significant enhancement of k_s was observed for FcAA with 24 hour adsorption. Additionally, the k_s of FcAA with 30 min adsorption was comparable to k_s of other modifiers with 30 min adsorptions (Table 2.4). Based on the observations, a change in the property of FcAA during the adsorption time was suspected, and aggregation of FcAA was hypothesized as the cause of the change. In literature, it is mentioned that aggregated phthalocyanines showed faster charge transfers than the monomers because the reorganization energy of the aggregates is smaller than that of the monomers.[93-95] If the aggregation of FcAA is relatively slow, it is possible that the majority of adsorbed FcAA with 30 min adsorption are monomers and those with 24 hour adsorption are aggregates. This may explain the difference in the charge transfer rate between the two different adsorption times. Additionally, if the hypothetical aggregation of FcAA is valid, it can be another factor that is responsible for the redox potential shift of FcAA in

Table 2.3. The aggregation is assumed to be produced via hydrogen bonding between the acid groups. The hydrogen bonding between molecules is also possible for the other modifiers. However, the hydrogen bonding between FcAAs may be stabilized via the interaction between methylenes in FcAAs, so that FcAAs might form aggregates while the other modifiers do not form aggregates. This hypothesis can be tested using absorption spectroscopy. If monomers and aggregates have distinguishable absorption wavelengths, the presence of each component and the relative amount of the component can be determined.

The charge transfer rates of FcAA, FcCA, FcHA, and FcPA are generally comparable except for FcAA with 24 hour adsorption. However, the charge transfer rates of FcSA are slightly lower than the others in both 30 min and 24 hour adsorptions. This may be because the electronic coupling between FcSA and ITO is relatively weaker than the others. According to Marcus theory, the charge transfer rate is proportional to the square of the electronic coupling matrix element (H_{AB}), which reflects the strength of the electronic coupling between the electron donor and the electron acceptor.[96-98] Unlike the dissolved molecule experiments, the modifiers are chemically bound to the surface of the electrode. Since the

modifiers are composed of Fc with different binding groups, the degree of electronic coupling between the modifier and ITO is assumed to vary depending on binding group, which leads to the variation in the charge transfer rate of the adsorbed modifiers. The electronic structures of modifier–ITO complexes can be simulated using the density functional theory.[99] The simulation would likely give more information about the electronic coupling between ITO and each modifier with different binding groups.

2.3.3 Charge transfer rate of solution probe (Fc) with modified electrodes

In Section 1.2.1, a model system using a solution electroactive probe was suggested to estimate the impact of the electrode modification on the charge collection efficiency (η_{CC}) of the electrode. To assess if the electrode modification alters the charge transfer rate of a solution probe, CVs were measured with unmodified and modified electrodes in the presence of the solution electroactive probe (Fc). Measured charge transfer rate constants of Fc with different electrodes are summarized in Table 2.5. The electroactive surface coverages and the redox potentials of the adsorbed layers, which were previously measured, are also listed in the table.

Table 2.5 Summary of charge transfer rate constants of solution probe (Fc) with unmodified and modified electrodes using 24 hr adsorptions, electroactive surface coverages and redox potentials of the adsorbed layers.

Modifier	Unmodified	FcAA	FcCA	FcHA	FcPA	FcSA
$10^3 k°$ (cm/s)	2.1 ± 0.1	4.3 ± 0.1	3.7 ± 0.7	4.4 ± 0.1	4.5 ± 0.1	2.9 ± 0.5
$10^{10}\Gamma$ (mol/cm^2)*	–	0.6 ± 0.1	0.7 ± 0.1	1.05 ± 0.07	2.9 ± 0.3	1.1 ± 0.4
$E_{1/2}$ (V)	0.098 ± 0.003[a]	0.09 ± 0.01[b]	0.32 ± 0.01[b]	0.27 ± 0.01[b]	0.11 ± 0.02[b]	0.31 ± 0.02[b]

* The electroactive surface coverages (values are taken from Table 2.2). [a] Redox potential of 1 mM Fc in 0.1 M TBAP/ACN. [b] Redox potentials of adsorbed layers for 24 hr adsorptions that were measured with 0.1 M TBAP/ACN (values are taken from Table 2.3).

The charge transfer rate constants (k°) for the solution probe (Fc) were generally enhanced with modified electrodes as shown in Table 2.5. The results agree with the results that were reported by Carter et al.[22] They modified ITO with the modifiers that contain carboxylic acid or dicarboxylic acid binding group and observed the enhancement of the charge transfer rate of a solution probe (Fc) with the modified ITO compared to the unmodified ITO.

When the redox reactions of the adsorbed molecules can mediate the charge transfer reaction of the free molecules in solution, the charge transfer rate of the solution probe can be enhanced. The adsorbed molecule mediated

charge transfer is illustrated in Figure 2.14. In order to be a good electrocatalyst, the redox potential of adsorbed molecules is expected to be close to the redox potential of the free molecules in solution since it can lower the free energy of the electrocatalysis reaction.[100] Contradictorily, the closeness of the redox potential of the adsorbed molecules to the redox potential of the free molecules in solution may also reduce the probability of the electrocatalysis reaction. For instance, in case of the oxidation reaction, electron transfer from the adsorbed modifier to the electrode is an essential prerequisite for the electrocatalysis reaction (the electron transfer from the solution probe to the oxidized form of the adsorbed modifier). However, if the redox potentials of the adsorbed modifier and the solution probe are close, the electron transfer from the solution probe to the electrode can almost concurrently occur with the electron transfer from the adsorbed modifier to the electrode. Thus, the probability of the electron transfer from the solution probe to the oxidized form of the adsorbed modifier may be lower than the case, which the redox potential of the adsorbed modifier is far more negative from the redox potential of the solution probe. Because of the contradictory effects, it is difficult to predict which adsorbed modifier would likely have the higher degree of the electrocatalytic effect based on the redox

potential of adsorbed modifier. Moreover, the electroactivation of the ITO surface is another possible cause of the enhancement of the charge transfer rate of the solution probe on modified electrodes. Consequently, evaluating the impact of the electrocatalytic effect of adsorbed modifier on the enhancement on the charge transfer rate of the solution probe could not be assessed unless the degree of the electroactivation of each modifier is known.

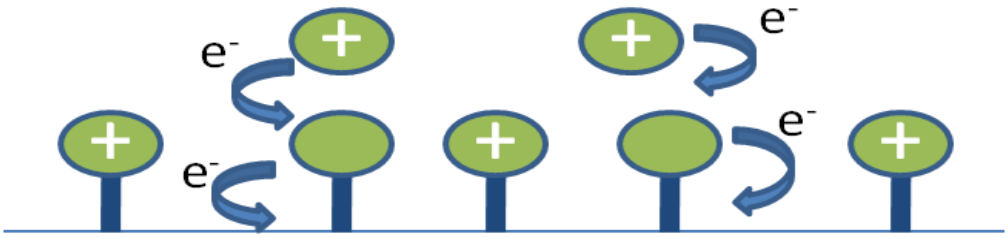

Figure 2.14 Illustration of the charge transfer of the solution probe mediated by the adsorbed modifiers. The picture describes a case of the oxidation reaction (e^- is an electron).

The electroactivation of the ITO surface by modifiers can also be responsible for the enhancement in the charge transfer rate of the solution probe with the modified electrodes. The relative degree of the electroactivation can be expected from the electroactive surface coverage of

each modifier if all electroactive sites are occupied by the modifiers. However, since there is no evidence, which suggests that all electroactive sites are occupied, it is difficult to determine which modifier would likely have the higher degree of the electroactivation.

Because the electrocatalytic effect and the electroactivation can concurrently be responsible for the enhancement in the charge transfer rate of the solution probe, and no clear expected results were present for the both factors, a discrete evaluation of the impact of each factor on the charge transfer rate of Fc could not be assessed. Modifications of TCOs using modifiers that contain a non-electroactive terminal group might allow a discrete evaluation of the electroactivation. The electrocatalytic effect was suspected since the modifiers used in this study have ferrocene, which is an electroactive molecule, as the terminal group. If an alkyl group such as CH_3 is used as the terminal group of the modifiers instead of ferrocene, the change in the charge transfer rate of the solution probe could be assigned solely to the surface electroactivation by modifiers. Additionally, comparing the results from modifiers having non-electroactive terminal groups and the results in Table 2.5 might allow us to analyze the impact of the electrocatalytic effect from ferrocene-containing modifiers on the charge

transfer rate of the solution probe. When the results are compared, the distance between a solution probe and the electrode needs to be taken into account since different terminal groups may vary the distance, and the electron transfer rate is dependent on the distance between an electron donor and acceptor according to the Marcus theory.[101-103] Using a surface sensitive spectroscopic technique, binding orientations of modifiers would be determined, which can be used to estimate the distance between a solution probe and the electrode.

2.4 Conclusion

In this chapter, modifications of the most widely used TCO, indium tin oxide (ITO), have been studied using cyclic voltammetry (CV). Investigations have been done with dissolved modifiers, adsorbed layers of modifiers, and the modified electrodes with a solution probe.

The charge transfer rates of dissolved modifiers were greater than the dissolved ferrocene. Electroactivation of the ITO surface by the modifiers is a likely cause. The redox potentials of dissolved modifiers generally showed a linear trend as a function of the Hammett constants of the acidic functional groups except FcCA and FcSA. The linear trend was also observed for the

adsorbed modifiers except FcPA. The solvents used for CV measurements were considered as limiting factors that determine the linear behavior of the modifiers. However, verification of this conclusion with other solvents remains to be done.

The electroactive surface coverage of the modifiers varied from ca. $0.6 – 2.9 \times 10^{10}$ mol/cm^2. The binding affinity, the binding orientation, and the electroactivation effect of a modifier were assumed to be related with the electroactive surface coverage. From the ranges of the surface coverage of close-packed monolayers that were theoretically calculated using a modeling program, it was shown that the binding orientation can have a contribution to the variation in the electroactive surface coverage. However, the effects of the binding affinity and the electroactivation on the electroactive surface coverage could not be determined conclusively.

The significant enhancement of the charge transfer rate of adsorbed FcAA was observed as a function of the adsorption time while the charge transfer rates of the other modifiers were independent of the adsorption time. Aggregation of FcAA was hypothesized to explain the enhancement in the charge transfer rate of FcAA.

The charge transfer rates of a solution electroactive probe (Fc) were measured with unmodified and modified ITOs. The charge transfer rates of Fc with modified ITOs were greater than that with unmodified ITO. The eletroactivation and the electrocatalytic effect of the modifiers were assumed to be the cause of the enhancement of the charge transfer rate of the solution probe.

3. EVALUATION OF SUBSTITUTED FERROCENE MODIFIERS ON IZO

3.1 Introduction

3.1.1 Investigation of an alternative TCO (IZO)

Among many different transparent conductive oxides (TCOs), indium tin oxide (ITO) has been the most widely used because of its electrical and optical properties that were stated in Section 2.1.1. However, in order to achieve the optimum electrical and optical properties, ITO needs to be crystallized, which requires high temperature (~ 300 °C) for the deposition process.[104, 105] Amorphous indium zinc oxide (IZO) is an attractive TCO for replacing ITO since it can be deposited at low temperature (< 50 °C) and shows comparable electrical conductivity and optical transparency to ITO.[105] Additionally, IZO has low compressive stress, which gives it the potential to be used in flexible devices.[106] However, many aspects of IZO that can be related to the device performance, such as the surface composition and structure, and the dependence of electric properties on the composition and structure, are not well understood.[107]

In order to assess the electrochemical properties of IZO and the effect of surface modification, electrochemical experiments similar to those done

with ITO were done with IZO. CVs of dissolved Fc were conducted with unmodified IZO to investigate the charge transfer between the redox active species with IZO versus ITO. FcCA and FcPA were used to modify the surface of IZO. The adsorbed layers were analyzed by CV, and the results were compared to the experiments performed using ITO. The charge transfer rate of a solution probe (Fc) at modified IZO was also investigated. Additionally, the adsorption of FcPA on nano-structured IZO was investigated to see how altering the morphology of the surface of IZO affects the adsorption and charge transfer rate of a modifier.

3.2 Experimental

The IZO-coated planar electrodes (sample "leybsld") used in this study were provided by Ajaya Sigdel at National Renewable Energy Laboratory (NREL). IZO targets (80/20 wt. % In_2O_3/ZnO) were used to deposit films by sputtering at ambient temperature, resulted in the coating thickness of $\leq$ 100 nm and a sheet resistance of ca. 66 Ω/sq.

The nano-structured, IZO-coated electrodes were provided by Akram Amooali Khosroabadi in College of Optical Sciences at University of Arizona. Polyacrylonitrile (PAN) pillars were deposited on the top of a glass

substrate, and then IZO was deposited on the top of the PAN pillars/glass substrate.[108] PAN pillars had a diameter of 180 ± 10 nm and a height of 290 ± 12 nm. The preparation of PAN pillars/glass substrates were performed by Akram Amooali Khosroabadi, and the IZO depositions were performed by Ajaya Sigdel at NREL. For IZO depositions, the same method and condition were used as those for the planar IZO electrodes that were described in the previous paragraph.

Commercially available ferrocene (Fluka), ferrocenecarboxylic acid (FcCA, ScienceLab), and ferrocenephosphonic acid (FcPA) synthesized by O'Neil Smith in Department of Chemistry and Biochemistry at Georgia Institute of Technology, were used. The molecules were the same as those used for the ITO experiments described in Chapter 2. A teflon electrochemical cell (electrode area: 0.673 cm^2) was used for solution probe CV experiments. A small teflon electrochemical cell (electrode area: 0.158 cm^2) was used for adsorbed layer experiments due to the limited IZO supply. All electrochemical measurements were performed on a CH Instruments Electrochemical Workstation (CHI420A). The second scan of the CV was used for all reported values and calculations unless otherwise noted. A 0.1 M tetrabutylammonium perchlorate (TBAP, Aldrich) in acetonitrile

(ACN,EMD) was used as supporting electrolyte. A Basi Non-Aqueous Reference Electrode kit was used for all experiments. A 0.01 M silver nitrate ($AgNO_3$) in the 0.1 M TBAP solution was used as the filling solution for the $Ag/AgNO_3$ reference electrode. The potential of the reference electrode is 0.351 V vs. a normal hydrogen electrode (NHE).[67]

3.2.1 Adsorbed layer experiments

All CV experiments for adsorbed layers were done with a scan rate of 0.1 V/sec. The electrolyte solution was 0.1 M TBAP/ACN and the reference electrode filling solution was 0.01 M $AgNO_3$ in 0.1 M TBAP/ACN. A potential range for scanning was chosen to be wide enough to determine the starting and ending point of peaks. The potential windows were -0.3 – 0.9 V and -0.5 – 0.5 V for FcCA and FcPA respectively.

3.2.1.1 Cleaning of IZO slides

IZO slides were cleaned by gentle rubbing with nitrile gloves with 1% Triton X-100 solution for 1 min, then sonicating for 10 min each in 1% Triton X-100, nanopure water, and ethanol. After ethanol sonication, the

slides were dried with nitrogen flow. Lastly, air plasma (Harrick model PDC-3XG) cleaning/activating was conducted for 10 min at 30 W.

3.2.1.2 Adsorbed layer formation

The 1 mM solutions of FcCA and FcPA were used to form the adsorbed layers on IZO. The solvent used in the adsorption process was ethanol. Cleaned IZO slides were soaked in each solution (40 mL), contained in a glass Coplin staining jar, for 24 hr.

The concentration of the adsorbed layer formation solution was varied with constant adsorption time (24 hr) for the adsorption isotherm experiments. The range of concentration was 10 µM – 5 mM and 0.1 µM – 5 mM for FcCA and FcPA respectively. Cleaned IZO slides were soaked in each solution (~ 20 mL), contained in a 20 mL beaker, covered with parafilm for 24 hr. All adsorbed layer formations were done in the room temperature (~ 25 °C).

3.2.1.3 Post-treatment

IZO slides were removed from the adsorbed layer formation solution after specified adsorption times and rinsed with the pure solvent that was used in the adsorption step. After the rinse, sonication was done in the pure solvent for 5 min to remove physisorbed molecules or contaminants.

3.2.2 Solution probe experiments

Solution probe (Fc) was dissolved in 0.1 M TBAP/ACN to prepare 1 mM solution. The reference electrode filling solution was 0.01 M $AgNO_3$ in 0.1 M TBAP/ACN. CV experiments were performed for modified (24 hr adsorption of each modifier) and unmodified ITO electrodes using Fc solution probe. Scan rates of CV experiments were 0.1, 0.5, or 1 V/sec. A potential range for scanning was chosen to be wide enough to determine the peak potential at the highest scan rate. The potential window of was -0.6 – 1.2 V for all experiments.

3.2.3 Nano-structured IZO experiments

In order to avoid the delamination of the IZO/PAN layer, the solution washing/sonicating steps were omitted from the cleaning procedure. Only air

plasma (Harrick model PDC-3XG) cleaning/activating was conducted for 1 min at medium power. The 1 mM FcPA in ethanol was used for the adsorptions of FcPA on the nano-structured IZO. In order to avoid the delamination, the solution contact area was controlled to be smaller than the area of the IZO/PAN film. The volume of the 1 mM FcPA solution contacted with the nano-structured IZO was ~ 2 mL. After 24 hour adsorption, the solution contact area of the nano-structured IZO was rinsed with pure ethanol, and then dried with nitrogen flow. CV was conducted after the drying. CVs were measure using the same conditions that were described in Section 3.2.1 except the potential window. The potential window was -1.0 – 1.0 V for the nano-structured IZO experiments.

3.3 Results and Discussion

3.3.1 Solution probe CV with unmodified IZO

In order to evaluate the intrinsic electroactivity of the surface of IZO, CV of the solution probe (Fc) on unmodified IZO was conducted, and it was compared to the same experiment with ITO. As shown in Figure 3.1, the peak separation from IZO is much greater than ITO. Using Nicholson

method, k° of Fc with IZO was calculated as $(1.4 \pm 0.5) \times 10^{-4}$ cm/s while k° of Fc with ITO was $(2.1 \pm 0.1) \times 10^{-3}$ cm/s.

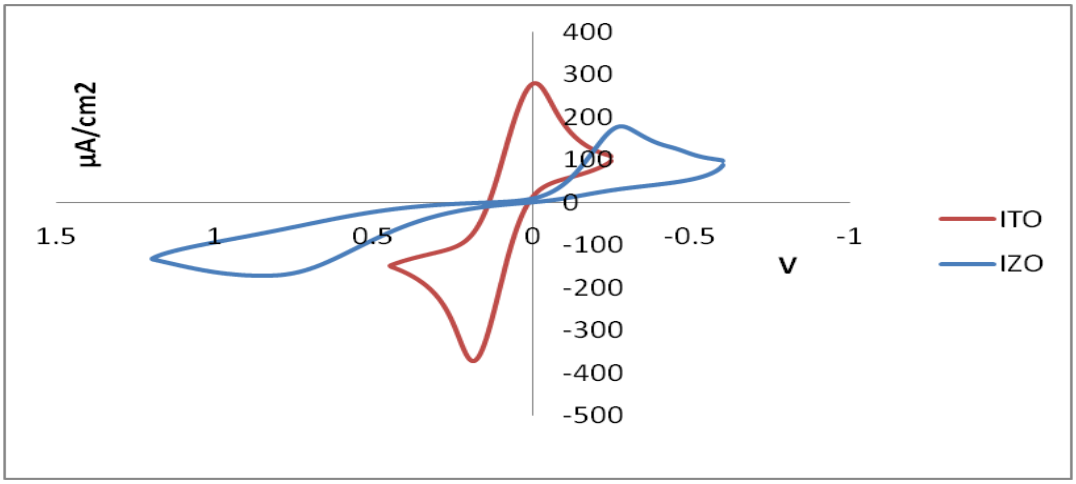

Figure 3.1 Cyclic voltammograms of 1 mM ferrocene in 0.1 M TBAP/ACN on unmodified ITO vs. unmodified IZO at 0.1 v/s scan rate.

The conductivity of IZO was determined to be ~ 2500 S/cm by Ajaya Sigdel at National Renewable Energy Laboratory who provided the IZO, whereas the conductivity of ITO was estimated as > 4000 S/cm from the product specifications provided by Colorado Concept Coatings LLC. If the surface electroactivity is directly correlated with the bulk conductivity, the difference in the conductivity may be a cause of the difference in the charge

transfer rate of Fc with IZO and with ITO. In case of metal electrodes, it was reported that the charge transfer rates of solution redox probes, such as benzoquinone and naphthoquinone, measured with gold electrode were comparable to those measured with platinum electrode[109] even though their conductivities are different (gold: 4.4×10^5 S/cm, platinum: 9.3×10^4 S/cm).[110] However, charge transfer rate on semiconductor electrodes is commonly observed as slower than that on metals, and low density of charge carriers has been suggested as a possible cause,[111-114] which can be associated with the conductivity of material.

Amorphous structure of IZO is also assumed to be a possible cause of the slower charge transfer rate of Fc on IZO compared to that on ITO. Popovich et al. investigated charge transfer kinetics on amorphous ITO and polycrystalline ITO.[115] They observed that the charge transfer rates of solution redox probes (tris(2,2′-bipyridyl ruthenium(II) chloride, ferrocyanide, and ferrocenemethanol) were generally slower on amorphous ITO compared to those on polycrystalline ITO. They attributed the difference to a greater density of defects sites along the grain boundaries and defect sites associated with substitutional tin in the crystalline lattice, which may be present in the crystalline ITO but not in the amorphous ITO. This

explanation may also be applied for the difference in the charge transfer rate of Fc between crystalline ITO and amorphous IZO since amorphous IZO does not contain above mentioned defects.

Additionally, relative amount of indium hydroxide species and oxygen defects at the surface of ITO and IZO can be responsible for the difference in the charge transfer rate. Figure 3.2 shows AFM height images and conductive tip AFM (C-AFM) images of the surface of ITO and IZO. The C-AFM images suggest that there is a noticeable difference in the surface electroactivity between IZO and ITO. Since indium oxide is the predominant component for both ITO (ca. 90%) and IZO (ca. 80%), the presence of $In(OH)_3$ was expected at the surface of IZO as it was present on the surface of ITO. The indium hydroxide species on the surface of IZO can be a cause of the electroinactivity as in the case of ITO. Additionally, in IZO electrodes, the free charge carriers (electrons) have been thought to be produced by oxygen defects as they are in the case of ITO.[116-119] Thus, If the amount of indium hydroxide species at the surface of IZO is relatively higher and/or the amount of the oxygen defects at the surface of the IZO is relatively lower, the surface of IZO can be more electroinactive than the surface of ITO. Gliboff et al. analyzed the x-ray photoemission spectroscopy

(XPS) data of oxygen plasma treated amorphous IZO (> 90% In) surface using a O (1s) model that was used for analysis of the ITO surface in the previous study.[3, 120] From the XPS data, they observed the peak that can be attributed to the hydroxide species (InOOH / $In(OH)_3$). Additionally, the relative percent composition of the hydroxide species was higher than that of the oxygen vacancy-like species. On the other hand, Donley et al. showed that the air plasma treated crystalline ITO surface has more oxygen vacancy-like species than the hydroxide species.[3] However, a quantitative comparison for the amount of $In(OH)_3$ and oxygen defects at the surface of IZO and ITO is not available from those results. Moreover, details of the cleaning/pretreatment method, the manufacturer of ITO, and the wt. % of In_2O_3 vs. ZnO of IZO in the literature are not exactly same for those in this study. Thus, XPS measurements on the exact electrodes used in this study are necessary to determine if $In(OH)_3$ and oxygen defects at the surface of IZO and ITO are responsible for difference in electroactivity.

Among the previously discussed factors that could possibly be related to the charge transfer rate of Fc, indium hydroxide species is associated with θ in Equation 2.1 while the others are more likely associated with $k^\circ_{0.}$ In other words, when a completely electroactive ITO is compared to a

completely electroactive IZO, it is possible that there is still a difference in the charge transfer rate of a solution probe.

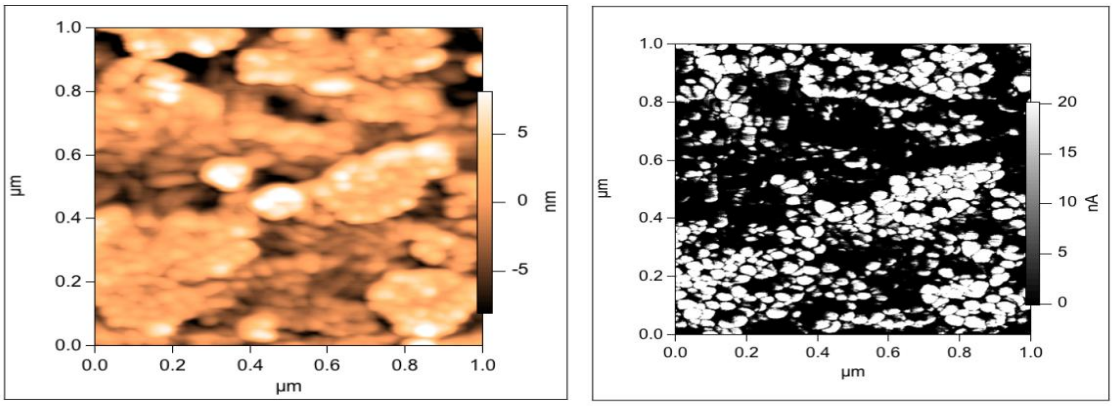

(a)

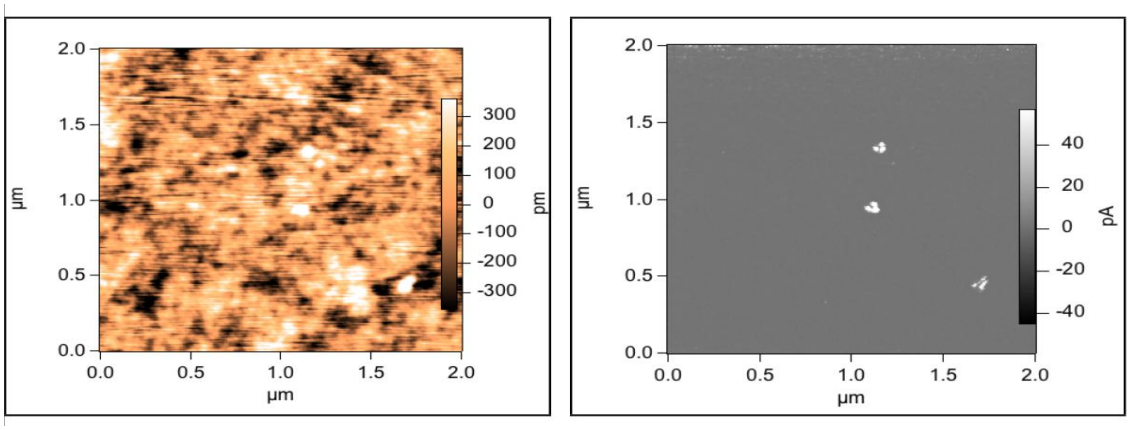

(b)

Figure 3.2 AFM images of ITO (a) and IZO (b). The images on the left are contact mode height images, and the images on the right are C-AFM

characterizations. (Images were provided by Ajaya Sigdel at National Renewable Energy Laboratory).

3.3.2 Adsorbed layers on IZO

FcCA and FcPA were used to modify the surface of IZO. CVs were conducted after modification to investigate the electroactive surface coverage, redox potential and charge transfer rate, of the adsorbed layers. The results are summarized in Table 3.1, and compared with the results of the same modifiers on ITO.

Table 3.1 Summary of adsorbed FcCA and FcPA layers on IZO vs. ITO.

	IZO		ITO	
	FcCA	FcPA	FcCA	FcPA
$10^{10}\Gamma$ (mol/cm^2)	0.6 ± 0.2	2.3 ± 0.5	0.7 ± 0.1	2.9 ± 0.3
Binding constant (M^{-1})	(1.1 ± 0.7) × 10^4	(3.0 ± 0.8) × 10^6	(3.8 ± 0.7) × 10^3	(2.8 ± 0.5) × 10^6
$E_{1/2}$ (V)	0.25 ± 0.04	0.04 ± 0.02	0.32 ± 0.01	0.11 ± 0.02
Chrage transfer rate (s^{-1})	0.5 ± 0.3	1.7 ± 0.4	3 ± 1	2.0 ± 0.2

The binding affinity, binding orientation, and electroactivation, which were evaluated for the electroactive modifier films on ITO, were also investigated for the electroactive film of FcCA and FcPA on IZO. The

electroactive surface coverage of FcPA was approximately four times larger than the electroactive surface coverage of FcCA, and the binding constant of FcPA on IZO was noticeably greater ($> \times 10^2$) than FcCA. Based on the observation, the binding constants of the modifiers on IZO seem to be correlated with the electroactive surface coverages. However, the correlation may not be vaild if the other modifiers are additionally investigated. In case of ITO, no clear dependence of the binding constant on the electroactive surface coverage was observed when all modifiers were compared (Section 2.3.2.2).

The effect of the binding orientation on the electroactive surface coverage was evaluated using the theoretical surface coverage of the close-packed monolayers of FcCA and FcPA in Table 2.2. The ranges of the close-packed monolayer coverages suggest that the binding orientation can vary the coverage. However, the binding orientation was not considered as the only factor that determines the electroactive surface coverage since the electroactive surface coverage measured for FcPA was ca. 4 times larger than FcCA while the maximum theoretical surface coverage of a close-packed monolayer of FcPA is only ca. 1.4 times larger than the minimum theoretical surface coverage of a close-packed monolayer of FcCA.

The electroactivation of the surface of IZO was also assumed to be related to the electroactive surface coverages of FcCA and FcPA. The degree of the electroactivation by FcCA and FcPA was expected to be estimated from the solution probe experiments in Section 3.3.3 since the electroactivation of the surface can alter the charge transfer rate of the solution probe. However, like as the case of ITO, the electroactivation and the electrocatalytic effect of the modifiers could not be distinguished. Thus, an evaluation of the relationship between the electroactivation and the electroactive surface coverage could not be assessed.

Redox potentials of both FcCA and FcPA adsorbed layers on IZO are ca. 70 mV less positive than those on ITO (Table 3.1). During a CV measurement, the Fermi level of the electrode can be altered by applying potential, and the oxidation of the modifier can occur when the Fermi level of the electrode is aligned with the HOMO level of the modifier. Since the Fermi level of electrode is defined by applied potential in CV experiment, the difference in redox potential suggests that the HOMO level of the adsorbed modifier on IZO is different from the HOMO level of the adsorbed modifier on ITO. It is assumed that the electronic structure of adsorbed

modifier varies because the modifier-IZO interaction is different from the modifier-ITO interaction.

The difference in the charge transfer rate of adsorbed modifiers was thought to be due to the difference in the electronic coupling strength between the adsorbed modifier and the electrode depending on binding group, as mentioned in Section 2.3.2.4. Based on the results in Table 3.1, FcCA seems to have a weaker electronic coupling with IZO relative to the electronic coupling of FcPA with IZO while the strength of the electronic coupling of FcCA and FcPA are assumed to be similar in the case of ITO. The degree of the electronic coupling is assumed to vary with different binding modes.[121] The binding modes of phosphonic acid on IZO was suggested as a mixture of bidentate and tridentate[120] while bidentate was assumed as a major binding mode of phosphonic acid on ITO in Section 2.3.2.2. From this, the binding mode of carboxylic acid on IZO is thought to be possibly different from that on ITO. Thus, the relative electronic coupling strength of FcCA and FcPA on IZO can be different from those on ITO.

The electroactive surface coverages of FcCA and FcPA on IZO were comparable to those on ITO (Table 3.1). The binding affinity, binding orientation, and the electroactivation were considered as possible factors that

vary the electroactive surface coverages on both IZO and ITO. Based on the comparable electroactive surface coverages, it was assumed that the summation of the effect from each factor for the modifiers on IZO is similar with that on ITO even though the effect of each individual factor could not be compared.

The electroactive surface coverages of adsorbed FcCA and FcPA on IZO decreased as more sequential scanning conducted, which was previously observed in the case of ITO. As shown in Figure 3.3, the FcPA adsorbed on IZO is more stable than the FcCA adsorbed on IZO. As it was mentioned in Section 2.3.2.2, the main binding mode of the modifier was assumed to be related with the stability. Using near edge x-ray absorption fine structure (NEXAFS) spectroscopy, polarization modulation infrared reflection absorption spectroscopy (PM-IRRAS), and x-ray photoelectron spectroscopy (XPS), Gliboff et al. investigated the adsorption of phenylphosphonic acid on amorphous IZOs.[120] They suggested that the binding modes of the phosphonic acid are a mixture of bidentate and tridentate. Assuming that the binding mechanisms of carboxylic acid on IZO surface are similar to those of phosphonic acid on IZO surface, the binding modes of carboxylic acid on IZO can be expected to be a mixture of

monodentate and bidentate. Since multiple bonds are expected to immobilize the modifiers more tightly onto the surface than a single bond, the FcPA on IZO can be more stable than the FcCA on IZO.

Even though the major binding mode of phosphonic acid on ITO was suggested as bindentate[86] while that on IZO was suggested as a mixture of bidentate and tridentate,[120] the stability of FcPA on IZO was comparable to the stability of FcPA on ITO (Figure 3.3). IZO and ITO have difference chemical compositions. Additionally, ITO is crystalline, which has long range order for its constituents whereas IZO is amorphous that has no long range order for its constituents. Thus, the binding energy of a modifier can be different for ITO and IZO even if the modifier adsorbs on both TCOs with the same binding mode. On the other hand, the binding energy of the modifier can be comparable with different binding mode on each TCO, which can lead to the comparable stability of the modifier on ITO and IZO.

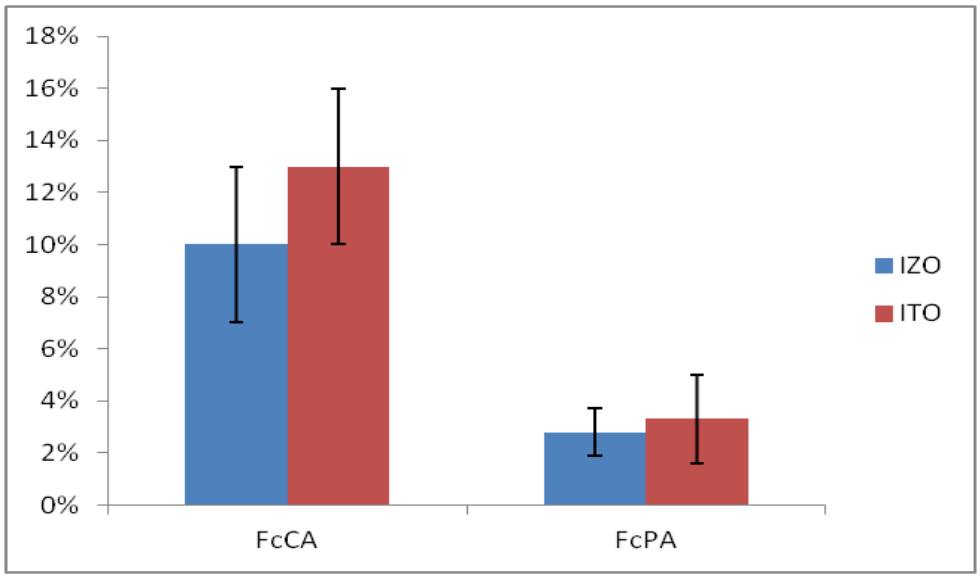

Figure 3.3 Surface coverage loss at 10th scan of CV for adsorbed layers on IZO vs. ITO prepared from 24 hour adsorption.

3.3.3 Charge transfer rate of solution probe (Fc) with modified electrodes

In order to assess the impact of the modification on IZO electrode and to compare it with the modified ITO electrodes, CVs were conducted with modified IZO electrodes in the presence of the solution electroactive probe (Fc). The charge transfer rate constant (k°) of Fc for FcCA modified IZO was $(2.9 \pm 0.7) \times 10^{-4}$ cm/s, and it was $(1.3 \pm 0.3) \times 10^{-3}$ for FcPA modified IZO. Both of the values are greater than the k° of Fc with unmodified IZO, $(1.4 \pm 0.5) \times 10^{-4}$ cm/s. The result suggests that the modification of the IZO electrode is effective to improve the surface charge transfer reaction, which

is consistent with ITO data discussed in Section 2.3.3. The enhancement of the charge transfer rate of Fc for FcPA modified IZO was noticeably greater than the enhancement for FcCA modified IZO while the enhancement for FcCA modified ITO was comparable to FcPA modified ITO (Section 2.3.3). The relatively higher degree of the enhancement for FcPA modified IZO is assumed to be either because the electroactivation by FcPA is greater than FcCA or because the electrocatalytic effect of adsorbed FcPA is greater than the adsorbed FcCA. However, as discussed in Section 2.3.3, the electrocatalytic effect and the electroactivation can concurrently be involved in the enhancement of the charge transfer rate, and the discrete evaluation of each effect could not be assessed based on the given data. The experiments using non-electroactive terminal group containing modifiers that were discussed in Section 2.3.3 would likely allow us to determine which effect is more responsible for the different degree of the enhancement.

3.3.4 Nano-structured IZO (nano-IZO)

A brief investigation was done to examine the adsorption of FcPA on nano-IZO. Nano-IZO electrodes were made and provided by collaborators (Akram Amooali Khosroabadi in College of Optical Sciences at University

of Arizona and Ajaya Sigdel at NREL). As shown in Figure 3.4, polyacrylonitrile (PAN) pillars were used to alter the surface morphology of the IZO electrode. The hypothesis to be examined was that the morphology of the surface of IZO affects the surface coverage of the modifier and possibly the charge transfer rate of adsorbed modifiers.

The results of adsorbed FcPA on nano-IZO are summarized in Table 3.2. For comparison, the results of adsorbed FcPA on regular IZO are also listed in the table, which is marked as "regular." In the cleaning procedure for nano-IZO, solution cleaning and sonicating steps were omitted to avoid possible delamination or degradation of the polymer (PAN) layer. Because of this, additional experiments were conducted with regular IZO, which was cleaned using the same procedure used for the nano-IZO. The results for those experiments are marked as "control."

As shown in the Table 3.2, the electroactive surface coverages and the charge transfer rates of FcPA on "flat" IZO with different cleaning procedures are comparable. Thus, it is assumed that the effect of a different cleaning procedure is not significant. The electro active surface coverage of FcPA on nano-IZO is about 8 ("control") – 10 ("regular") times higher than that on IZO. The difference in the electroactive surface coverage of FcPA is

close to the difference in the exposed surface between nano-IZO and “flat” IZO. Using the ImageJ program, it was estimated that the surface area of the nano-IZO is about 7.6 times higher than the surface area of the “flat” IZO (data provided by Akram Amooali Khosroabadi in College of Optical Sciences at University of Arizona).

The charge transfer rate of the FcPA on nano-IZO was noticeably lower than the charge transfer rate of FcPA on IZO. The conductivity of the nano-IZO is ~ 1700 S/cm, which is lower than the conductivity of IZO (~ 2500 S/cm). If the surface electroactivity is directly correlated with the bulk conductivity, the difference can be a reason for the lower charge transfer rate of FcPA on nano-IZO. However, there are other factors that may be related to the charge transfer rate such as indium hydroxide species, surface oxygen defects, and heterogeneity of the surface. Additionally, the compatibility of IZO layer to PAN pillars used in nano-IZO may not be the same as the compatibility of IZO layer to glass substrate. More investigations on nano-IZO regarding those factors would likely give more information to explain the slow charge transfer rate of FcPA on nano-IZO.

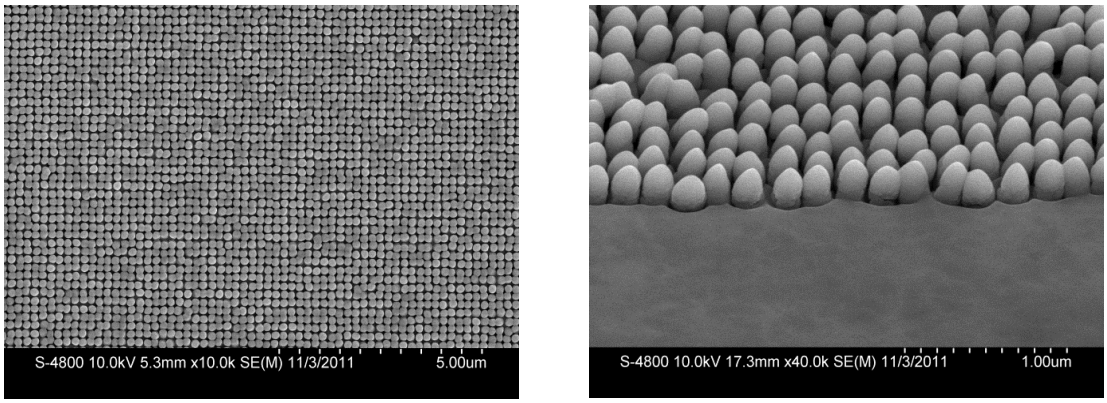

(a) (b)

Figure 3.4 FE-SEM images of nano-structured IZO. (a) is the top view and (b) is the side view of an IZO substrate. (Images were provided by Akram Amooali Khosroabadi in College of Optical Sciences at University of Arizona).

Table 3.2 Summary of electroactive surface coverages and charge transfer rate constants of FcPA on "flat" and nano-structured IZO.

IZO type	Γ ($\times 10^{-10}$ mol/cm^2)	k_s (s^{-1})
Regular[a]	2.3 ± 0.5	1.7 ± 0.4
Control[b]	3.0 ± 0.5	1.9 ± 0.1
Nano-structured	24.3 ± 5.3	0.8 ± 0.3

[a] "Flat" IZO using regular cleaning procedure. [b] "Flat" IZO using the cleaning procedure for nano-structured IZO.

3.4 Conclusion

In this chapter, the electrochemical properties of indium zinc oxide (IZO) and the effect of the IZO modifications using FcCA and FcPA have been studied. The results from CV measurements on IZO were also compared with those on ITO. Additionally, the adsorption of FcPA on nano-structured IZO was investigated.

The charge transfer rate of a solution redox probe (Fc) with unmodified IZO was much lower ($< \times 0.1$) than that with ITO. The bulk conductivity, the indium hydroxide species at the surface, and the oxygen defects at the surface were considered as possible factors that cause the difference in the charge transfer rate of Fc for ITO and IZO.

Adsorbed layers of FcCA and FcPA on IZO were investigated and compared with those on ITO. The electroactive surface coverages of the modifiers on IZO were comparable to those on ITO. The redox potentials of the adsorbed FcCA and FcPA on IZO were ca. 70 mV more negative than those on ITO. It can be either because of the difference in the work function of ITO and IZO or because of the difference in molecule-electrode interactions. Thus, the measurement of the work function of both electrodes is desirable.

The charge transfer rate of the solution probe (Fc) was higher with modified IZOs using FcCA and FcPA than that with unmodified IZO. The charge transfer rate of Fc with FcPA modified IZO was greater than that with FcCA modified IZO while comparable charge transfer rates of Fc were observed for FcCA modified ITO and FcPA modified ITO. The electroactivation and the electrocatalytic effect of the modifiers were assumed to generate the enhancement in the charge transfer rate of Fc. However, the evaluation of the individual effect could not be assessed. Investigations on the modifications using modifiers having non-electroactive terminal groups may allow us to analyze the individual effect separately.

The adsorbed layer of FcPA on nano-structured IZO was investigated. The enhancement in the electroactive surface coverage compared to the adsorption on “flat” IZO was comparable to the enhancement in the exposed surface area between nano-IZO and “flat” IZO. The charge transfer rate of adsorbed FcPA on nano-IZO was significantly lower than that of FcPA on IZO. Even though a conclusive explanation for the cause was not found, the results suggest that the change in the surface morphology can alter the electroactive surface coverage and the charge transfer rate of adsorbed modifiers.

4. CONCLUSION AND FUTURE DIRECTIONS

4.1 Conclusion

Several substituted ferrocenes, which have different acidic functional groups as substituents, were used to modify TCO (ITO and IZO) surfaces. Using an electrochemical technique (cyclic voltammetry), the modified electrodes were evaluated to see whether the modifications alter the charge transfer kinetics at the surface of the electrodes. For both ITO and IZO, the charge transfer rate of a solution probe (Fc) was greater on modified electrodes than that on unmodified electrodes. The presence of indium hydroxide species at the surface of electrodes is assumed to generate electroinactive regions on the electrodes. The indium hydroxide species is thought to be complexed with modifiers and removed from the surface (electroactivation of the surface of the electrode). The electroactivation can be contributed to the enhancement of the charge transfer rate of a solution probe on modified electrodes. However, the electrocatalytic effect of the adsorbed modifiers can also be responsible for the enhancement of the charge transfer rate of the solution probe. Because the two effects could not be evaluated separately, the relative degree of the electroactivation by each modifier could not be determined. Nevertheless, the results suggest that the

modification of TCO has a potential to enhance the charge collection efficiency of TCO electrode.

4.2 Future directions

Adsorptions of the modifiers that have a non-electroactive terminal group are desirable. Using a solution electroactive probe, the charge transfer rate at the electrode before and after the modification could be compared. When adsorbed modifiers do not have an electroactive moiety, the change in the charge transfer rate of the solution probe could be attributed to the electroactivation. The results from the non-electroactive modifiers would be compared to the previously obtained results from the solution probe experiments of ITO and IZO. The impact of electrocatalytic effect of Fc containing modifiers might be evaluated from the comparison. The distance between a solution probe and the electrode needs to be taken into account for the comparison since the distance may vary depending on the terminal group, and the electron transfer rate is dependent on the distance. Binding orientation of each modifier and the distance between a solution probe and the electrode would possibly be investigated using a spectroscopic technique such as photoelastic modulation infrared reflection absorption spectroscopy

(PM-IRRAS). More information on the electroactivation and the binding orientation of each modifier would then be used for seeking a determining factor that varies the electroactive surface coverage of different modifiers.

The surface of ITO and IZO will be investigated using x-ray photoemission spectroscopy (XPS). Quantitative data might be obtained for the indium hydroxide species and the oxygen defects at the surface of ITO and IZO. This would allow us to have a better understanding about the difference in the charge transfer rate of a solution probe and adsorbed modifiers between ITO and IZO.

Adsorptions of the other modifiers on nano-IZO will be performed. Solution probe experiments will also be performed on modified nano-IZO to see if the modification has a similar effect for the electrode that has a controlled morphology. PM-IRRAS and XPS studies will also be conducted for modified nano-IZO.

In addition to the modifiers that used in this study, the modifiers containing different length of alkyl chains in between Fc and binding group will be studied. Different results might be observed in many aspects such as the binding orientation, electroactive surface coverage, and the contact resistance depending on the length of the spacer. The impact of the

modification using new modifiers on the charge transfer rate at the electrode would be evaluated using CV and compared to the previous data.

APPENDIX A. ANALYSIS OF DISSOLVED MOLECULE CV EXPERIMENTS

Figure A.1 illustrates a typical cyclic voltammogram observed for a diffusion controlled experiment. E_{pa} and E_{pc} in the diagram represent the anodic peak potential and the cathodic peak potential. In this study, all CV experiments were controlled by CHI420A software. The peak potentials can be determined using the program. The redox potential was determined as the midpoint potential between E_{pa} and E_{pc}. Additionally, peak separation (ΔE_p) was determined as $\left|E_{pa} - E_{pc}\right|$.

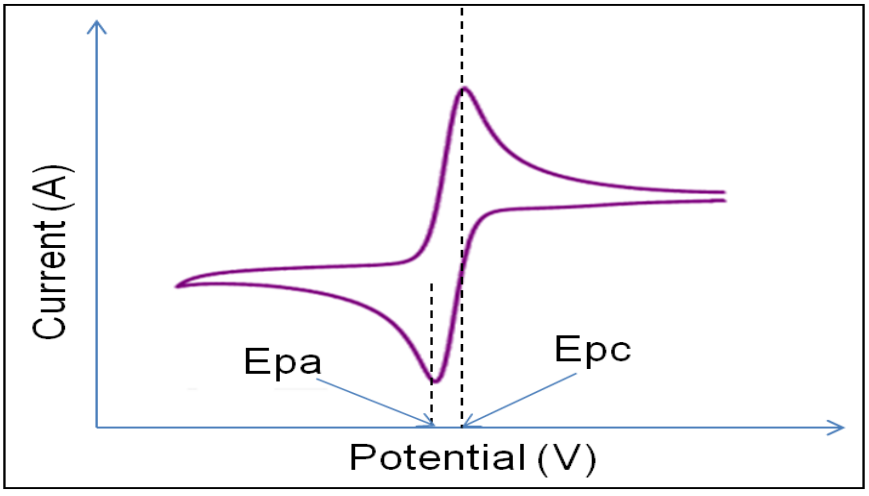

Figure A.1 A typical cyclic voltammogram for the diffusion controlled experiments.

In 1965, Nicholson introduced a method to evaluate the charge transfer rate of diffusion controlled electroactive species.[122] He described the relationship between the standard rate constant (k°) and the dimensionless parameter ψ as shown in the following equation.

$$\psi = \frac{(\frac{D_O}{D_R})^{\alpha/2} k^0}{\sqrt{\pi a D_O}} \qquad (a=nF\nu/RT) \qquad (A.1)$$

where D, n, F, ν, R, and T are diffusion coefficient, number of charges involved in the reaction, Faraday's constant, scan rate, gas constant, and temperature respectively. Additionally, the variation of the value of ψ as a function of peak separation (ΔE_p) was provided (Table A.1).

ψ	$n\Delta E_p$ (mV)
20	61
7	63
6	64
5	65
4	66
3	68
2	72
1	84
0.75	92
0.5	105
0.35	121
0.25	141
0.1	212

Table A.1 Variations of the kinetic parameter depending on the peak potential separation.[122] (Adapted from Ref. 122).

As shown in Figure A.2, the data was plotted using the Origin8 program, and the equation for the fitted curve was determined to be

$$\psi = 24.248/(n\Delta E_p - 59.785) \qquad (A.2)$$

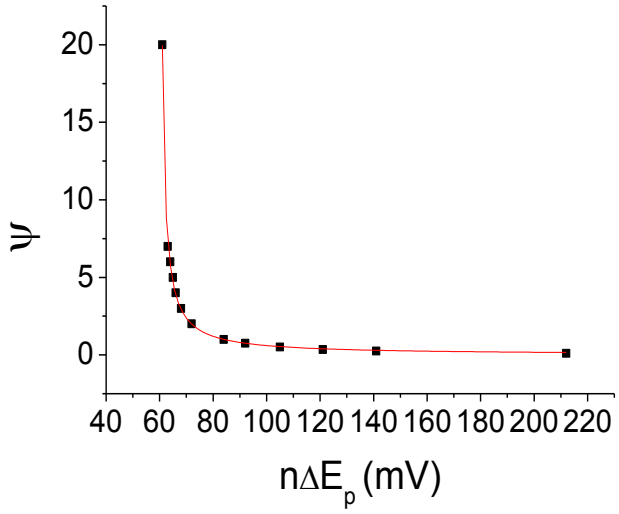

Figure A.2 The plot of the kinetic parameter (ψ) vs. peak separation (ΔE_p) based on the data provided in Nicholson's paper.[122]

Thus, the value of ψ can be extrapolated from the experimental ΔE_p value. When constants of Equation A.1 are summarized in a parameter C, the equation can be written as

$$\psi = Ck^0\nu^{-0.5} \qquad (A.3)$$

The plot of ψ vs. $\nu^{-0.5}$ can be generated by varying scan rates, and the value of k^0 can then be obtained from the slope of the linear plot. Figure A.3, shows example plots for dissolved molecules.

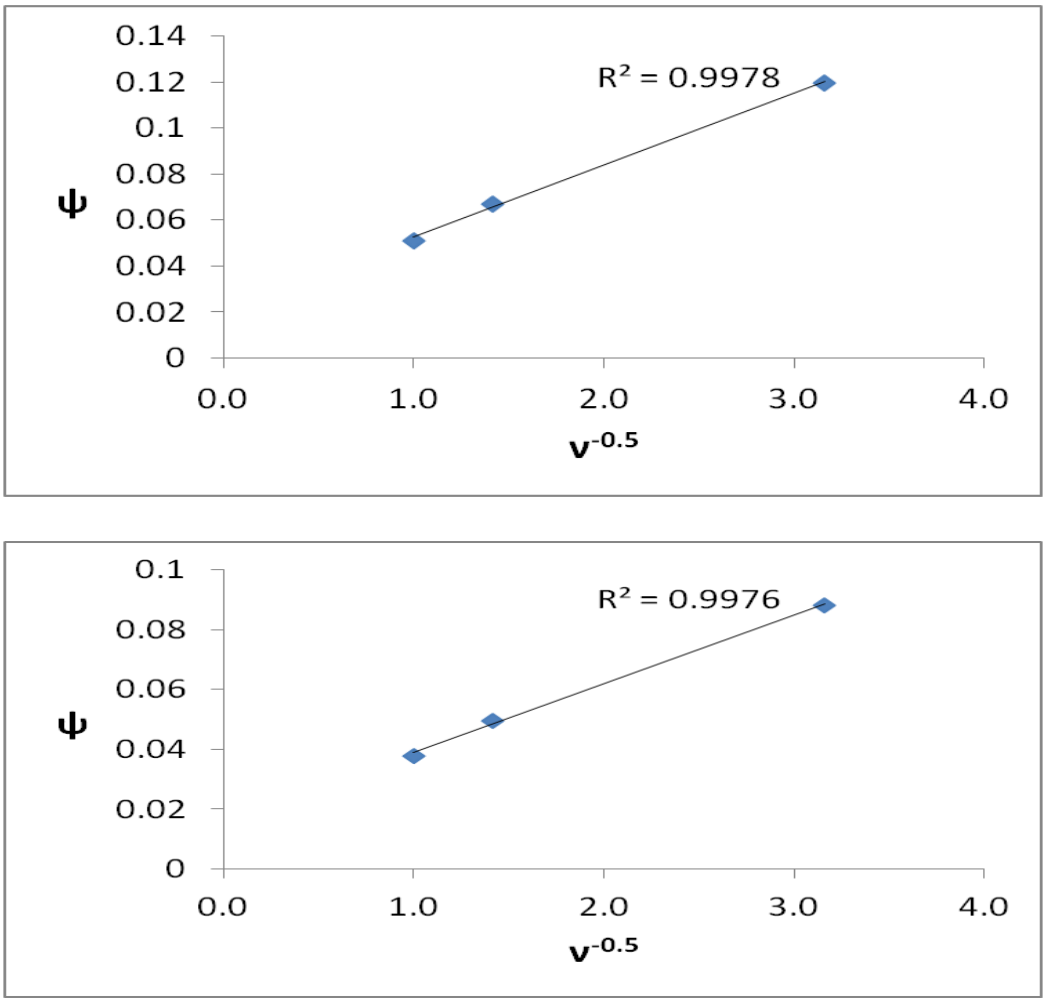

Figure A.3 Plots of ψ vs. $\nu^{-0.5}$ for dissolved FcCA (top) and FcPA (bottom).

APPENDIX B. ANALYSIS OF ADSORBED LAYER CV EXPERIMENTS

Figure B.1 illustrates a typical cyclic voltammogram observed for a strongly adsorbed electroactive species on the surface of an electrode. E_{pa} and E_{pc} in the diagram represent the anodic peak potential and the cathodic peak potential. In this study, all CV experiments were controlled by CHI420A software. The peak potentials can be determined using the program. The redox potential was determined as the midpoint potential between E_{pa} and E_{pc}. Additionally, peak separation (ΔE_p) was determined as $\left|E_{pa} - E_{pc}\right|$. Additionally, the electroactive surface coverage of the adsorbed molecules on the surface can be calculated using the following equation.[52]

$$\Gamma = Q/nFA \qquad \text{(B.1)}$$

where Γ is the electroactive surface coverage, Q is the charge involved in the reaction that can be determined by integrating the area under the peak, n is the number of electrons transferred, F is Faraday's constant, and A is the electrode area.

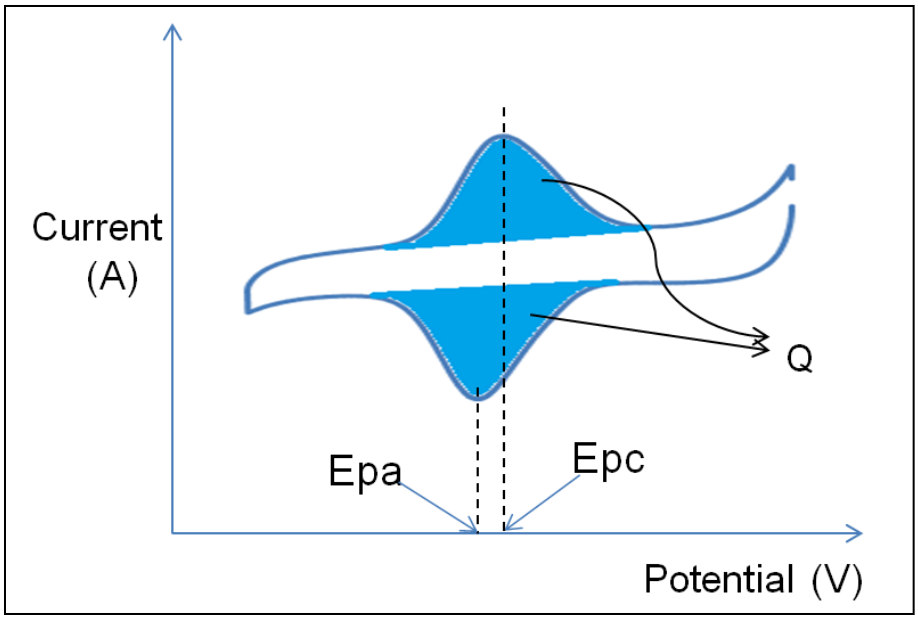

Figure B.1 A typical cyclic voltammogram for the strongly adsorbed electroactive species.

In 1979, Laviron introduced a method to evaluate the charge transfer rate of strongly adsorbed electroactive species.[123] He described the relationship between the heterogeneous rate constant (k_s) and the dimensionless parameter m as shown in the following equation.

$$m = \left(\frac{RT}{F}\right)(k_s/n\nu) \qquad (B.2)$$

where R is the gas constant, T is temperature, F is Faraday's constant, n is the number of electrons, and ν is the scan rate. Additionally, the variation of

the value of 1/m as a function of peak separation (ΔE_p) was provided (Table B.1).

1/m	$n\Delta E_p$ (mV)
0.5	18.8
0.75	27
1	34.8
1.5	48.8
2	61.2
2.5	72.2
3	82.4
3.5	91.8
4	100.6
6	130
7	142.4
8	153.8
9	164
10	173.4
11	182
12	190
13	197.6
14	204.6

Table B.1 Variations of the dimensionless parameter depending on the peak potential separation.[123] (Adapted from Ref. 123).

As shown in Figure B.2, the data was plotted using the Microsoft Excel program, and the equation for the fitting curve was determined to be

$$\frac{1}{m} = -1.12 \times 10^{-13}x^6 + 8.11 \times 10^{-11}x^5 - 2.02 \times 10^{-8}x^4 + 2.79 \times 10^{-6}x^3 - 2.75 \times 10^{-5}x^2 + 2.81 \times 10^{-2}x - 3.39 \times 10^{-2} \quad \text{(B.3)}$$

($x = n\Delta E_p$)

Thus, the value of 1/m can be extrapolated from the experimental ΔE_p value. The heterogeneous rate constant (k_s) can then be determined using Equation B.2.

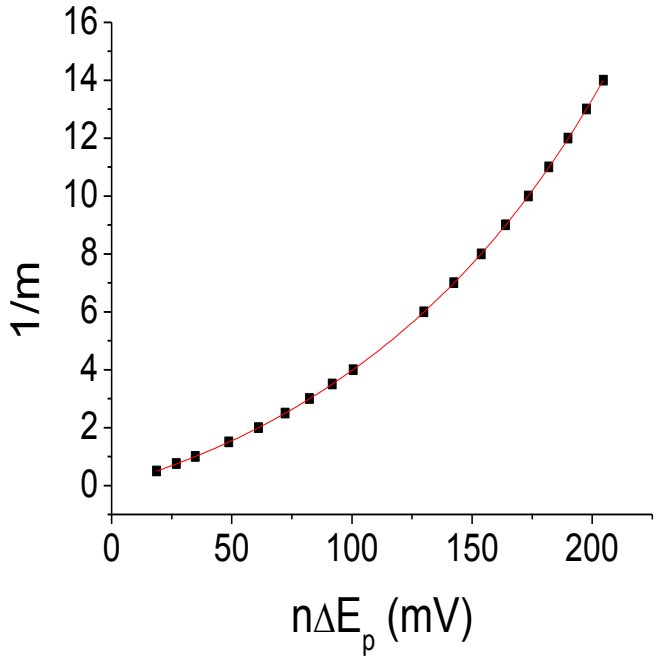

Figure B.2 The plot of the dimensionless parameter (1/m) vs. peak separation (ΔE_p) based on the data provided in Laviron's paper.[123]

APPENDIX C. COPYRIGHT PERMISSIONS

AMERICAN INSTITUTE OF PHYSICS LICENSE TERMS AND CONDITIONS

Aug 07, 2012

License Number	2963931294863
Order Date	Aug 07, 2012
Publisher	American Institute of Physics
Publication	Journal of Applied Physics
Article Title	Small molecular weight organic thin-film photodetectors and solar cells
Author	Peter Peumans, Aharon Yakimov, Stephen R. Forrest
Online Publication Date	Apr 1, 2003
Volume number	93
Issue number	7
Type of Use	Thesis/Dissertation
Requestor type	Student
Format	Print and electronic
Portion	Figure/Table
Number of figures/tables	1
Title of your thesis / dissertation	Electrochemical Evaluation of TCO modifications Using Substituted Ferrocenes
Expected completion date	Aug 2012
Estimated size (number of pages)	120
Total	0.00 USD

Terms and Conditions

American Institute of Physics -- Terms and Conditions: Permissions Uses

American Institute of Physics ("AIP") hereby grants to you the non-exclusive right and license to use and/or distribute the Material according to the use

specified in your order, on a one-time basis, for the specified term, with a maximum distribution equal to the number that you have ordered. Any links or other content accompanying the Material are not the subject of this license.

1. You agree to include the following copyright and permission notice with the reproduction of the Material: "Reprinted with permission from [FULL CITATION]. Copyright [PUBLICATION YEAR], American Institute of Physics." For an article, the copyright and permission notice must be printed on the first page of the article or book chapter. For photographs, covers, or tables, the copyright and permission notice may appear with the Material, in a footnote, or in the reference list.
2. If you have licensed reuse of a figure, photograph, cover, or table, it is your responsibility to ensure that the material is original to AIP and does not contain the copyright of another entity, and that the copyright notice of the figure, photograph, cover, or table does not indicate that it was reprinted by AIP, with permission, from another source. Under no circumstances does AIP, purport or intend to grant permission to reuse material to which it does not hold copyright.
3. You may not alter or modify the Material in any manner. You may translate the Material into another language only if you have licensed translation rights. You may not use the Material for promotional purposes. AIP reserves all rights not specifically granted herein.
4. The foregoing license shall not take effect unless and until AIP or its agent, Copyright Clearance Center, receives the Payment in accordance with Copyright Clearance Center Billing and Payment Terms and Conditions, which are incorporated herein by reference.
5. AIP or the Copyright Clearance Center may, within two business days of granting this license, revoke the license for any reason whatsoever, with a full refund payable to you. Should you violate the terms of this license at any time, AIP, American Institute of Physics, or Copyright Clearance Center may revoke the license with no refund to you. Notice of such revocation will be made using the contact information provided by you. Failure to receive such notice will not nullify the revocation.
6. AIP makes no representations or warranties with respect to the Material. You agree to indemnify and hold harmless AIP, American Institute of Physics, and their officers, directors, employees or agents from and against any and all claims arising out of your use of the Material other than as specifically authorized herein.
7. The permission granted herein is personal to you and is not transferable or assignable without the prior written permission of AIP. This license may not be amended except in a writing signed by the party to be charged.
8. If purchase orders, acknowledgments or check endorsements are issued on any forms containing terms and conditions which are inconsistent with these provisions, such inconsistent terms and conditions shall be of no force and effect. This document, including the CCC Billing and Payment Terms and Conditions, shall be the entire agreement between the parties relating to the subject matter hereof.

This Agreement shall be governed by and construed in accordance with the laws of the State

of New York. Both parties hereby submit to the jurisdiction of the courts of New York County for purposes of resolving any disputes that may arise hereunder.

AMERICAN INSTITUTE OF PHYSICS LICENSE TERMS AND CONDITIONS

Aug 07, 2012

License Number	2963940563164
Order Date	Aug 07, 2012
Publisher	American Institute of Physics
Publication	Journal of Applied Physics
Article Title	X-ray photoemission spectroscopy studies of Sn-doped indium-oxide films
Author	John C. C. Fan, John B. Goodenough
Online Publication Date	Aug 1, 1977
Volume number	48
Issue number	8
Type of Use	Thesis/Dissertation
Requestor type	Student
Format	Print and electronic
Portion	Figure/Table
Number of figures/tables	1
Title of your thesis / dissertation	Electrochemical Evaluation of TCO modifications Using Substituted Ferrocenes
Expected completion date	Aug 2012
Estimated size (number of pages)	120
Total	0.00 USD

Terms and Conditions

American Institute of Physics -- Terms and Conditions: Permissions Uses

American Institute of Physics ("AIP") hereby grants to you the non-exclusive right and license to use and/or distribute the Material according to the use specified in your order, on a one-time basis, for the specified term, with a maximum distribution equal to the number that you have ordered. Any links or other content accompanying the Material are not the subject of this license.

1. You agree to include the following copyright and permission notice with the reproduction of the Material: "Reprinted with permission from [FULL CITATION]. Copyright [PUBLICATION YEAR], American Institute of Physics." For an article, the copyright and permission notice must be printed on the first page of the article or book chapter. For photographs, covers, or tables, the copyright and permission notice may appear with the Material, in a footnote, or in the reference list.
2. If you have licensed reuse of a figure, photograph, cover, or table, it is your responsibility to ensure that the material is original to AIP and does not contain the copyright of another entity, and that the copyright notice of the figure, photograph, cover, or table does not indicate that it was reprinted by AIP, with permission, from another source. Under no circumstances does AIP, purport or intend to grant permission to reuse material to which it does not hold copyright.
3. You may not alter or modify the Material in any manner. You may translate the Material into another language only if you have licensed translation rights. You may not use the Material for promotional purposes. AIP reserves all rights not specifically granted herein.
4. The foregoing license shall not take effect unless and until AIP or its agent, Copyright Clearance Center, receives the Payment in accordance with Copyright Clearance Center Billing and Payment Terms and Conditions, which are incorporated herein by reference.
5. AIP or the Copyright Clearance Center may, within two business days of granting this license, revoke the license for any reason whatsoever, with a full refund payable to you. Should you violate the terms of this license at any time, AIP, American Institute of Physics, or Copyright Clearance Center may revoke the license with no refund to you. Notice of such revocation will be made using the contact information provided by you. Failure to receive such notice will not nullify the revocation.
6. AIP makes no representations or warranties with respect to the Material. You agree to indemnify and hold harmless AIP, American Institute of Physics, and their officers, directors, employees or agents from and against any and all claims arising out of your use of the Material other than as specifically authorized herein.
7. The permission granted herein is personal to you and is not transferable or assignable without the prior written permission of AIP. This license may not be amended except in a writing signed by the party to be charged.
8. If purchase orders, acknowledgments or check endorsements are issued on any forms containing terms and conditions which are inconsistent with these provisions, such inconsistent terms and conditions shall be of no force and effect. This document,

including the CCC Billing and Payment Terms and Conditions, shall be the entire agreement between the parties relating to the subject matter hereof.

This Agreement shall be governed by and construed in accordance with the laws of the State of New York. Both parties hereby submit to the jurisdiction of the courts of New York County for purposes of resolving any disputes that may arise hereunder.

Copyright Clearance Center RightsLink®

ACS Publications High quality. High impact.

Logged in as:
Saehan Park
LOGOUT

Title: Characterization of Indium−Tin Oxide Interfaces Using X-ray Photoelectron Spectroscopy and Redox Processes of a Chemisorbed Probe Molecule: Effect of Surface Pretreatment Conditions

Author: Carrie Donley et al.

Publication: Langmuir

Publisher: American Chemical Society

Date: Jan 1, 2002

Copyright © 2002, American Chemical Society

PERMISSION/LICENSE IS GRANTED FOR YOUR ORDER AT NO CHARGE

This type of permission/license, instead of the standard Terms & Conditions, is sent to you because no fee is being charged for your order. Please note the following:

- Permission is granted for your request in both print and electronic formats, and translations.
- If figures and/or tables were requested, they may be adapted or used in part.
- Please print this page for your records and send a copy of it to your publisher/graduate school.
- Appropriate credit for the requested material should be given as follows: "Reprinted (adapted) with permission from (COMPLETE REFERENCE CITATION). Copyright (YEAR) American Chemical Society." Insert appropriate information in place of the capitalized words.
- One-time permission is granted only for the use specified in your request. No additional uses are granted (such as derivative works or other editions). For any other uses, please submit a new request.

Copyright Clearance Center RightsLink®

ACS Publications High quality. High impact.

Logged in as:
Saehan Park
LOGOUT

Title: The Modification of Indium Tin Oxide with Phosphonic Acids: Mechanism of Binding, Tuning of Surface Properties, and Potential for Use in Organic Electronic Applications

Author: Peter J. Hotchkiss, Simon C. Jones, Sergio A. Paniagua, Asha Sharma, Bernard Kippelen, Neal R. Armstrong, and Seth R. Marder

Publication: Accounts of Chemical Research

Publisher: American Chemical Society

Date: Mar 1, 2012

Copyright © 2012, American Chemical Society

PERMISSION/LICENSE IS GRANTED FOR YOUR ORDER AT NO CHARGE

This type of permission/license, instead of the standard Terms & Conditions, is sent to you because no fee is being charged for your order. Please note the following:

- Permission is granted for your request in both print and electronic formats, and translations.
- If figures and/or tables were requested, they may be adapted or used in part.
- Please print this page for your records and send a copy of it to your publisher/graduate school.
- Appropriate credit for the requested material should be given as follows: "Reprinted (adapted) with permission from (COMPLETE REFERENCE CITATION). Copyright (YEAR) American Chemical Society." Insert appropriate information in place of the capitalized words.

- One-time permission is granted only for the use specified in your request. No additional uses are granted (such as derivative works or other editions). For any other uses, please submit a new request.

Copyright Clearance Center RightsLink®

ACS Publications High quality. High impact.

Title: Theory and Application of Cyclic Voltammetry for Measurement of Electrode Reaction Kinetics.

Author: R. S. Nicholson

Publication: Analytical Chemistry

Publisher: American Chemical Society

Date: Oct 1, 1965

Copyright © 1965, American Chemical Society

Logged in as:

Saehan Park

Account #:

3000556543

LOGOUT

PERMISSION/LICENSE IS GRANTED FOR YOUR ORDER AT NO CHARGE

This type of permission/license, instead of the standard Terms & Conditions, is sent to you because no fee is being charged for your order. Please note the following:

- Permission is granted for your request in both print and electronic formats, and translations.
- If figures and/or tables were requested, they may be adapted or used in part.
- Please print this page for your records and send a copy of it to your publisher/graduate school.
- Appropriate credit for the requested material should be given as follows: "Reprinted (adapted) with permission from (COMPLETE REFERENCE CITATION). Copyright (YEAR) American Chemical Society." Insert appropriate information in place of the capitalized words.
- One-time permission is granted only for the use specified in your request. No additional uses are granted (such as derivative works or other editions). For any other uses, please submit a new request.

ELSEVIER LICENSE
TERMS AND CONDITIONS

Aug 08, 2012

This is a License Agreement between Saehan Park ("You") and Elsevier ("Elsevier") provided by Copyright Clearance Center ("CCC"). The license consists of your order details, the terms and conditions provided by Elsevier, and the payment terms and conditions.

Supplier	Elsevier Limited The Boulevard,Langford Lane Kidlington,Oxford,OX5 1GB,UK
Registered Company Number	1982084
Customer name	Saehan Park
Customer address	4225 N 1st AVE Tucson, AZ 85719
License number	2964361304973
License date	Aug 08, 2012
Licensed content publisher	Elsevier
Licensed content publication	Journal of Electroanalytical Chemistry
Licensed content title	General expression of the linear potential sweep voltammogram in the case of diffusionless electrochemical systems
Licensed content author	E. Laviron
Licensed content date	25 July 1979
Licensed content volume number	101
Licensed content issue number	1

Number of pages	10
Start Page	19
End Page	28
Type of Use	reuse in a thesis/dissertation
Intended publisher of new work	other
Portion	figures/tables/illustrations
Number of figures/tables/illustrations	1
Format	both print and electronic
Are you the author of this Elsevier article?	No
Will you be translating?	No
Order reference number	
Title of your thesis/dissertation	Electrochemical Evaluation of TCO modifications Using Substituted Ferrocenes
Expected completion date	Aug 2012
Estimated size (number of pages)	120
Elsevier VAT number	GB 494 6272 12
Permissions price	0.00 USD
VAT/Local Sales Tax	0.0 USD / 0.0 GBP
Total	0.00 USD
Terms and Conditions	

INTRODUCTION

1. The publisher for this copyrighted material is Elsevier. By clicking "accept" in connection with completing this licensing transaction, you agree that the following terms and conditions apply to this transaction (along with the Billing and Payment terms and conditions established by Copyright Clearance Center, Inc. ("CCC"), at the time that you opened your Rightslink account and that are available at any time at http://myaccount.copyright.com).

GENERAL TERMS

2. Elsevier hereby grants you permission to reproduce the aforementioned material

subject to the terms and conditions indicated.

3. Acknowledgement: If any part of the material to be used (for example, figures) has appeared in our publication with credit or acknowledgement to another source, permission must also be sought from that source. If such permission is not obtained then that material may not be included in your publication/copies. Suitable acknowledgement to the source must be made, either as a footnote or in a reference list at the end of your publication, as follows:

"Reprinted from Publication title, Vol /edition number, Author(s), Title of article / title of chapter, Pages No., Copyright (Year), with permission from Elsevier [OR APPLICABLE SOCIETY COPYRIGHT OWNER]." Also Lancet special credit - "Reprinted from The Lancet, Vol. number, Author(s), Title of article, Pages No., Copyright (Year), with permission from Elsevier."

4. Reproduction of this material is confined to the purpose and/or media for which permission is hereby given.

5. Altering/Modifying Material: Not Permitted. However figures and illustrations may be altered/adapted minimally to serve your work. Any other abbreviations, additions, deletions and/or any other alterations shall be made only with prior written authorization of Elsevier Ltd. (Please contact Elsevier at permissions@elsevier.com)

6. If the permission fee for the requested use of our material is waived in this instance, please be advised that your future requests for Elsevier materials may attract a fee.

7. Reservation of Rights: Publisher reserves all rights not specifically granted in the combination of (i) the license details provided by you and accepted in the course of this licensing transaction, (ii) these terms and conditions and (iii) CCC's Billing and Payment terms and conditions.

8. License Contingent Upon Payment: While you may exercise the rights licensed immediately upon issuance of the license at the end of the licensing process for the transaction, provided that you have disclosed complete and accurate details of your proposed use, no license is finally effective unless and until full payment is received from you (either by publisher or by CCC) as provided in CCC's Billing and Payment terms and conditions. If full payment is not received on a timely basis, then any license preliminarily granted shall be deemed automatically revoked and shall be void as if never granted. Further, in the event that you breach any of these terms and conditions or any of CCC's Billing and Payment terms and conditions, the license is automatically revoked and shall be void as if never granted. Use of materials as described in a revoked license, as well as any use of the materials beyond the scope of an unrevoked license, may constitute copyright infringement and publisher reserves the right to take

any and all action to protect its copyright in the materials.

9. Warranties: Publisher makes no representations or warranties with respect to the licensed material.

10. Indemnity: You hereby indemnify and agree to hold harmless publisher and CCC, and their respective officers, directors, employees and agents, from and against any and all claims arising out of your use of the licensed material other than as specifically authorized pursuant to this license.

11. No Transfer of License: This license is personal to you and may not be sublicensed, assigned, or transferred by you to any other person without publisher's written permission.

12. No Amendment Except in Writing: This license may not be amended except in a writing signed by both parties (or, in the case of publisher, by CCC on publisher's behalf).

13. Objection to Contrary Terms: Publisher hereby objects to any terms contained in any purchase order, acknowledgment, check endorsement or other writing prepared by you, which terms are inconsistent with these terms and conditions or CCC's Billing and Payment terms and conditions. These terms and conditions, together with CCC's Billing and Payment terms and conditions (which are incorporated herein), comprise the entire agreement between you and publisher (and CCC) concerning this licensing transaction. In the event of any conflict between your obligations established by these terms and conditions and those established by CCC's Billing and Payment terms and conditions, these terms and conditions shall control.

14. Revocation: Elsevier or Copyright Clearance Center may deny the permissions described in this License at their sole discretion, for any reason or no reason, with a full refund payable to you. Notice of such denial will be made using the contact information provided by you. Failure to receive such notice will not alter or invalidate the denial. In no event will Elsevier or Copyright Clearance Center be responsible or liable for any costs, expenses or damage incurred by you as a result of a denial of your permission request, other than a refund of the amount(s) paid by you to Elsevier and/or Copyright Clearance Center for denied permissions.

LIMITED LICENSE

The following terms and conditions apply only to specific license types:

15. **Translation**: This permission is granted for non-exclusive world **English** rights only unless your license was granted for translation rights. If you licensed translation

rights you may only translate this content into the languages you requested. A professional translator must perform all translations and reproduce the content word for word preserving the integrity of the article. If this license is to re-use 1 or 2 figures then permission is granted for non-exclusive world rights in all languages.

16. **Website**: The following terms and conditions apply to electronic reserve and author websites:
Electronic reserve: If licensed material is to be posted to website, the web site is to be password-protected and made available only to bona fide students registered on a relevant course if:
This license was made in connection with a course,
This permission is granted for 1 year only. You may obtain a license for future website posting,
All content posted to the web site must maintain the copyright information line on the bottom of each image,
A hyper-text must be included to the Homepage of the journal from which you are licensing at http://www.sciencedirect.com/science/journal/xxxxx or the Elsevier homepage for books at http://www.elsevier.com , and
Central Storage: This license does not include permission for a scanned version of the material to be stored in a central repository such as that provided by Heron/XanEdu.

17. **Author website** for journals with the following additional clauses:

All content posted to the web site must maintain the copyright information line on the bottom of each image, and the permission granted is limited to the personal version of your paper. You are not allowed to download and post the published electronic version of your article (whether PDF or HTML, proof or final version), nor may you scan the printed edition to create an electronic version. A hyper-text must be included to the Homepage of the journal from which you are licensing at http://www.sciencedirect.com/science/journal/xxxxx . As part of our normal production process, you will receive an e-mail notice when your article appears on Elsevier's online service ScienceDirect (www.sciencedirect.com). That e-mail will include the article's Digital Object Identifier (DOI). This number provides the electronic link to the published article and should be included in the posting of your personal version. We ask that you wait until you receive this e-mail and have the DOI to do any posting.

Central Storage: This license does not include permission for a scanned version of the material to be stored in a central repository such as that provided by Heron/XanEdu.

18. **Author website** for books with the following additional clauses:
Authors are permitted to place a brief summary of their work online only.
A hyper-text must be included to the Elsevier homepage at http://www.elsevier.com .

All content posted to the web site must maintain the copyright information line on the bottom of each image. You are not allowed to download and post the published electronic version of your chapter, nor may you scan the printed edition to create an electronic version.

Central Storage: This license does not include permission for a scanned version of the material to be stored in a central repository such as that provided by Heron/XanEdu.

19. **Website** (regular and for author): A hyper-text must be included to the Homepage of the journal from which you are licensing at http://www.sciencedirect.com/science/journal/xxxxx. or for books to the Elsevier homepage at http://www.elsevier.com

20. **Thesis/Dissertation**: If your license is for use in a thesis/dissertation your thesis may be submitted to your institution in either print or electronic form. Should your thesis be published commercially, please reapply for permission. These requirements include permission for the Library and Archives of Canada to supply single copies, on demand, of the complete thesis and include permission for UMI to supply single copies, on demand, of the complete thesis. Should your thesis be published commercially, please reapply for permission.

REFERENCES

1. Peumans, P.; Yakimov, A.; Forrest, S. R., Small molecular weight organic thin-film photodetectors and solar cells. *Journal of Applied Physics* **2003,** *93* (7), 3693-3723.

2. Fan, J. C. C.; Goodenough, J. B., X-Ray Photoemission Spectroscopy Studies of Sn-Doped Indium-Oxide Films. *Journal of Applied Physics* **1977,** *48* (8), 3524-3531.

3. Donley, C.; Dunphy, D.; Paine, D.; Carter, C.; Nebesny, K.; Lee, P.; Alloway, D.; Armstrong, N. R., Characterization of indium-tin oxide interfaces using X-ray photoelectron spectroscopy and redox processes of a chemisorbed probe molecule: Effect of surface pretreatment conditions. *Langmuir* **2002,** *18* (2), 450-457.

4. Hotchkiss, P. J.; Jones, S. C.; Paniagua, S. A.; Sharma, A.; Kippelen, B.; Armstrong, N. R.; Marder, S. R., The Modification of Indium Tin Oxide with Phosphonic Acids: Mechanism of Binding, Tuning of Surface Properties, and Potential for Use in Organic Electronic Applications. *Accounts of Chemical Research 45* (3), 337-346.

5. Goetzberger, A.; Hebling, C.; Schock, H. W., Photovoltaic materials, history, status and outlook. *Materials Science & Engineering R-Reports* **2003,** *40* (1), 1-46.

6. Green, M. A., Photovoltaic principles. *Physica E-Low-Dimensional Systems & Nanostructures* **2002,** *14* (1-2), 11-17.

7. Gratzel, M., Photoelectrochemical cells. *Nature* **2001,** *414* (6861), 338-344.

8. Armstrong, N. R.; Veneman, P. A.; Ratcliff, E.; Placencia, D.; Brumbach, M., Oxide Contacts in Organic Photovoltaics: Characterization and Control of Near-Surface Composition in Indium-Tin Oxide (ITO) Electrodes. *Accounts of Chemical Research* **2009,** *42* (11), 1748-1757.

9. Ma, C. Z.; Peng, Y. Q.; Xie, H. W.; Wang, R. S.; Li, R. H.; Wang, Y.; Xie, J. P.; Yang, T., Numerical model for planar heterojunction organic solar cells on the condition of short circuit. *Materials Science and Engineering B-Advanced Functional Solid-State Materials* **2011,** *176* (5), 406-411.

10. Hoppe, H.; Sariciftci, N. S., Organic solar cells: An overview. *Journal of Materials Research* **2004,** *19* (7), 1924-1945.

11. Peters, C. H.; Sachs-Quintana, I. T.; Kastrop, J. P.; Beaupre, S.; Leclerc, M.; McGehee, M. D., High Efficiency Polymer Solar Cells with Long Operating Lifetimes. *Advanced Energy Materials* **2011,** *1* (4), 491-494.

12. Heliatek sets new world record efficiency of 10.7 % for its organic tandem cell. http://www.heliatek.com/?p=1923&lang=en.

13. Dimitrakopoulos, C. D.; Mascaro, D. J., Organic thin-film transistors: A review of recent advances. *Ibm Journal of Research and Development* **2001,** *45* (1), 11-27.

14. Kippelen, B.; Bredas, J. L., Organic photovoltaics. *Energy & Environmental Science* **2009,** *2* (3), 251-261.

15. Martin Pope, C. E. S., *Electronic Processes in Organic Crystals and Polymers*. 2nd edition ed.; Oxford University Press: New York, 1999.

16. Li, J. F.; Wang, L.; Liu, J.; Evmenenko, G.; Dutta, P.; Marks, T. J., Characterization of transparent conducting oxide surfaces using self-assembled electroactive monolayers. *Langmuir* **2008,** *24* (11), 5755-5765.

17. Brumbach, M.; Veneman, P. A.; Marrikar, F. S.; Schulmeyer, T.; Simmonds, A.; Xia, W.; Lee, P.; Armstrong, N. R., Surface composition and electrical and electrochemical properties of freshly deposited and acid-etched indium tin oxide electrodes. *Langmuir* **2007,** *23* (22), 11089-11099.

18. Snell, K. D.; Keenan, A. G., Surface modified electrodes. *Chemical Society Reviews* **1979,** *8* (2), 259-282.

19. Brumbach, M.; Armstrong, N. R., Modification of Transparent Conducting Oxide (TCO) Electrodes through Silanization and Chemisorption of Small Molecules. In *Encyclopedia of Electrochemistry*, Wiley-VCH Verlag GmbH & Co. KGaA: 2007.

20. Armstrong, N. R.; Veneman, P. A.; Ratcliff, E.; Placencia, D.; Brumbach, M., Oxide Contacts in Organic Photovoltaics: Characterization and Control of Near-Surface Composition in Indiumâˆ’Tin Oxide (ITO) Electrodes. *Accounts of Chemical Research* **2009,** *42* (11), 1748-1757.

21. Armstrong, N. R.; Carter, C.; Donley, C.; Simmonds, A.; Lee, P.; Brumbach, M.; Kippelen, B.; Domercq, B.; Yoo, S., Interface modification of ITO thin films: organic photovoltaic cells. *Thin Solid Films* **2003,** *445* (2), 342-352.

22. Carter, C.; Brumbach, M.; Donley, C.; Hreha, R. D.; Marder, S. R.; Domercq, B.; Yoo, S.; Kippelen, B.; Armstrong, N. R., Small molecule chemisorption on indium-tin oxide surfaces: enhancing probe molecule electron-transfer rates and the performance of organic light-emitting diodes. *Journal of Physical Chemistry B* **2006,** *110* (50), 25191-25202.

23. McNamara, W. R.; Milot, R. L.; Song, H. E.; Snoeberger, R. C.; Batista, V. S.; Schmuttenmaer, C. A.; Brudvig, G. W.; Crabtree, R. H., Water-stable, hydroxamate anchors for functionalization of TiO2 surfaces with ultrafast interfacial electron transfer. *Energy & Environmental Science* **2010,** *3* (7), 917-923.

24. Raman, A.; Quinones, R.; Barriger, L.; Eastman, R.; Parsi, A.; Gawalt, E. S., Understanding Organic Film Behavior on Alloy and Metal Oxides. *Langmuir* **2010,** *26* (3), 1747-1754.

25. Yee, C.; Kataby, G.; Ulman, A.; Prozorov, T.; White, H.; King, A.; Rafailovich, M.; Sokolov, J.; Gedanken, A., Self-assembled monolayers of alkanesulfonic and -phosphonic acids on amorphous iron oxide nanoparticles. *Langmuir* **1999,** *15* (21), 7111-7115.

26. Moss, J. A.; Yang, J. C.; Stipkala, J. M.; Wen, X. G.; Bignozzi, C. A.; Meyer, G. J.; Meyer, T. J., Sensitization and stabilization of TiO2

photoanodes with electropolymerized overlayer films of ruthenium and zinc polypyridyl complexes: A stable aqueous photoelectrochemical cell. *Inorganic Chemistry* **2004,** *43* (5), 1784-1792.

27. Love, J. C.; Estroff, L. A.; Kriebel, J. K.; Nuzzo, R. G.; Whitesides, G. M., Self-assembled monolayers of thiolates on metals as a form of nanotechnology. *Chemical Reviews* **2005,** *105* (4), 1103-1169.

28. Ray, B.; Nair, P. R.; Alam, M. A., Annealing dependent performance of organic bulk-heterojunction solar cells: A theoretical perspective. *Solar Energy Materials and Solar Cells* **2011,** *95* (12), 3287-3294.

29. Zhu, K.; Neale, N. R.; Miedaner, A.; Frank, A. J., Enhanced charge-collection efficiencies and light scattering in dye-sensitized solar cells using oriented TiO2 nanotubes arrays. *Nano Letters* **2007,** *7* (1), 69-74.

30. Randles, J. E. B., Kinetics of Rapid Electrode Reactions. *Discussions of the Faraday Society* **1947,** *1*, 11-19.

31. Vyas, R. N.; Wang, B., Electrochemical Analysis of Conducting Polymer Thin Films. *International Journal of Molecular Sciences* **2010,** *11* (4), 1956-1972.

32. Ho, C.; Raistrick, I. D.; Huggins, R. A., Application of Ac Techniques to the Study of Lithium Diffusion in Tungsten Trioxide Thin-Films. *Journal of the Electrochemical Society* **1980,** *127* (2), 343-350.

33. Tsierkezos, N. G.; Ritter, U., Electrochemical and thermodynamic properties of hexacyanoferrate(II)/(III) redox system on multi-walled carbon nanotubes. *The Journal of Chemical Thermodynamics* (0).

34. Sundfors, F.; Bobacka, J.; Ivaska, A.; Lewenstam, A., Kinetics of electron transfer between Fe(CN)(6)(3-/4-) and poly(3,4-ethylenedioxythiophene) studied by electrochemical impedance spectroscopy. *Electrochimica Acta* **2002,** *47* (13-14), 2245-2251.

35. Eckermann, A. L.; Feld, D. J.; Shaw, J. A.; Meade, T. J., Electrochemistry of redox-active self-assembled monolayers. *Coordination Chemistry Reviews* **2010,** *254* (15-16), 1769-1802.

36. Dunitz, J. D.; Orgel, L. E.; Rich, A., The Crystal Structure of Ferrocene. *Acta Crystallographica* **1956,** *9* (4), 373-375.

37. Seiler, P.; Dunitz, J. D., New Interpretation of the Disordered Crystal-Structure of Ferrocene. *Acta Crystallographica Section B-Structural Science* **1979,** *35* (May), 1068-1074.

38. Coriani, S.; Haaland, A.; Helgaker, T.; Jorgensen, P., The equilibrium structure of ferrocene. *Chemphyschem* **2006,** *7* (1), 245-249.

39. Zara, A. J.; Machado, S. r. S.; BulhÃµes, L. O. v. S.; Benedetti, A. V.; Rabockai, T., The electrochemistry of ferrocene in non-aqueous solvents. *Journal of Electroanalytical Chemistry and Interfacial Electrochemistry* **1987,** *221* (1â€“2), 165-174.

40. Sharp, M., Determination of the charge-transfer kinetics of ferrocene at platinum and vitreous carbon electrodes by potential steps chronocoulometry. *Electrochimica Acta* **1983,** *28* (3), 301-308.

41. Moharram, Y. I., Extraction of electrode kinetics and transport parameters of ferrocene at a platinum electrode from semiintegral electroanalysis. *Journal of Electroanalytical Chemistry* **2006,** *587* (1), 115-126.

42. Gagne, R. R.; Koval, C. A.; Lisensky, G. C., Ferrocene as an internal standard for electrochemical measurements. *Inorganic Chemistry* **1980,** *19* (9), 2854-2855.

43. Bond, A. M.; Henderson, T. L. E.; Mann, D. R.; Mann, T. F.; Thormann, W.; Zoski, C. G., A fast electron transfer rate for the oxidation of ferrocene in acetonitrile or dichloromethane at platinum disk ultramicroelectrodes. *Analytical Chemistry* **1988,** *60* (18), 1878-1882.

44. Armstrong, N. R.; Quinn, R. K.; Vanderborgh, N. E., Heterogeneous charge transfer rates of the ferrocene oxidation in sulfolane. [In sulfolane]. *Journal Name: J. Electrochem. Soc.; (United States); Journal Volume: 123:5* **1976**, Medium: X; Size: Pages: 646-649.

45. Tsierkezos, N., Cyclic Voltammetric Studies of Ferrocene in Nonaqueous Solvents in the Temperature Range from 248.15 to 298.15 K. *Journal of Solution Chemistry* **2007,** *36* (3), 289-302.

46. Pommerehne, J.; Vestweber, H.; Guss, W.; Mahrt, R. F.; Bässler, H.; Porsch, M.; Daub, J., Efficient two layer leds on a polymer blend basis. *Advanced Materials* **1995,** *7* (6), 551-554.

47. Tang, Q.; Tong, Y.; Hu, W.; Wan, Q.; Bjørnholm, T., Assembly of Nanoscale Organic Single-Crystal Cross-Wire Circuits. *Advanced Materials* **2009,** *21* (42), 4234-4237.

48. McNeill, C. R.; Halls, J. J. M.; Wilson, R.; Whiting, G. L.; Berkebile, S.; Ramsey, M. G.; Friend, R. H.; Greenham, N. C., Efficient Polythiophene/Polyfluorene Copolymer Bulk Heterojunction Photovoltaic Devices: Device Physics and Annealing Effects. *Advanced Functional Materials* **2008,** *18* (16), 2309-2321.

49. Shrotriya, V.; Li, G.; Yao, Y.; Chu, C. W.; Yang, Y., Transition metal oxides as the buffer layer for polymer photovoltaic cells. *Applied Physics Letters* **2006,** *88* (7).

50. Garrido, J. A.; RodrÃ-guez, R. M.; Bastida, R. M.; Brillas, E., Study by cyclic voltammetry of a reversible surface charge transfer reaction when the reactant diffuses to the electrode. *Journal of Electroanalytical Chemistry* **1992,** *324* (1â€“2), 19-32.

51. Eckermann, A. L.; Feld, D. J.; Shaw, J. A.; Meade, T. J., Electrochemistry of redox-active self-assembled monolayers. *Coordination Chemistry Reviews 254* (15â€“16), 1769-1802.

52. Bard, A. J.; Faulkner, L. R., *ELECTROCHEMICAL METHODS*. Second ed.; John Wiley & Sons, Inc.: New York, 2001.

53. Chemical Information Profile for Indium Tin Oxide. Services, U. S. D. o. H. a. H., Ed. Research Triangle Park, 2009.

54. Meng, L. J.; dos Santos, M. P., Study of the effect of the oxygen partial pressure on the properties of rf reactive magnetron sputtered tin-doped indium oxide films. *Applied Surface Science* **1997,** *120* (3-4), 243-249.

55. Yang, Y.; Jin, S.; Medvedeva, J. E.; Ireland, J. R.; Metz, A. W.; Ni, J.; Hersam, M. C.; Freeman, A. J.; Marks, T. J., CdO as the Archetypical Transparent Conducting Oxide. Systematics of Dopant Ionic Radius and Electronic Structure Effects on Charge Transport and Band Structure. *Journal of the American Chemical Society* **2005,** *127* (24), 8796-8804.

56. Balasubramanian, N.; Subrahmanyam, A., Electrical and Optical-Properties of Reactively Evaporated Indium Tin Oxide (Ito) Films - Dependence on Substrate-Temperature and Tin Concentration. *Journal of Physics D-Applied Physics* **1989,** *22* (1), 206-209.

57. Liau, Y. H.; Scherer, N. F.; Rhodes, K., Nanoscale electrical conductivity and surface spectroscopic studies of indium-tin oxide. *Journal of Physical Chemistry B* **2001,** *105* (16), 3282-3288.

58. Marikkar, F. S. MOLECULAR DESIGN OF ELECTRODE SURFACES AND INTERFACES: FOR OPTIMIZED CHARGE TRANSFER AT TRANSPARENT CONDUCTING OXIDE ELECTRODES AND SPECTROELECTROCHEMICAL SENSING Dissertation, UNIVERSITY OF ARIZONA 2006.

59. Zacher, B.; Armstrong, N. R., Modeling the Effects of Molecular Length Scale Electrode Heterogeneity in Organic Solar Cells. *Journal of Physical Chemistry C* **2011,** *115* (51), 25496-25507.

60. Amatore, C.; Saveant, J. M.; Tessier, D., Kinetics of Electron-Transfer to Organic-Molecules at Solid Electrodes in Organic Media. *Journal of Electroanalytical Chemistry* **1983,** *146* (1), 37-45.

61. Amatore, C.; Saveant, J. M.; Tessier, D., Charge-Transfer at Partially Blocked Surfaces - a Model for the Case of Microscopic Active and Inactive Sites. *Journal of Electroanalytical Chemistry* **1983,** *147* (1-2), 39-51.

62. Finklea, H. O.; Snider, D. A.; Fedyk, J.; Sabatani, E.; Gafni, Y.; Rubinstein, I., Characterization of Octadecanethiol-Coated Gold Electrodes as Microarray Electrodes by Cyclic Voltammetry and Ac-Impedance Spectroscopy. *Langmuir* **1993,** *9* (12), 3660-3667.

63. Holt, K. B.; Bard, A. J.; Show, Y.; Swain, G. M., Scanning electrochemical microscopy and conductive probe atomic force microscopy studies of hydrogen-terminated boron-doped diamond electrodes with different doping levels. *Journal of Physical Chemistry B* **2004,** *108* (39), 15117-15127.

64. Downs, A. J., *Chemistry of Aluminum, Gallium, Indium and Thallium*. Blackie Academic & Professional: Glasgow, 1993.

65. Narayanan, R.; Laine, R. M., Synthesis of soluble aluminium carboxylates directly from aluminium hydroxide. *Journal of Materials Chemistry* **2000,** *10* (9), 2097-2104.

66. Habeeb, J. J.; Tuck, D. G., Coordination-Compounds of Indium .21. Some Compounds Derived from Indium(Iii) Acetate, Including Indium Diacetate. *Journal of the Chemical Society-Dalton Transactions* **1973,** (3), 243-247.

67. Xu, W.; Peng, B.; Chen, J.; Liang, M.; Cai, F., New triphenylamine-based dyes for dye-sensitized solar cells. *Journal of Physical Chemistry C* **2008,** *112* (3), 874-880.

68. Mcdaniel, D. H.; Brown, H. C., An Extended Table of Hammett Substituent Constants Based on the Ionization of Substituted Benzoic Acids. *Journal of Organic Chemistry* **1958,** *23* (3), 420-427.

69. Emilia, M.; Silva, N. P. R. A.; Pombeiro, A. J. L.; Dasilva, J. J. R. F.; Herrmann, R.; Deus, N.; Bozak, R. E., Redox Potential and Substituent Effects in Ferrocene Derivatives .2. *Journal of Organometallic Chemistry* **1994,** *480* (1-2), 81-90.

70. Hoh, G. L.; Kleinberg, J.; Mcewen, W. E., Substituent Effects in Chronopotentiometric Oxidation of Ferrocenes. *Journal of the American Chemical Society* **1961,** *83* (19), 3949-&.

71. Silva, M. E. N. P. R. A.; Pombeiro, A. J. L.; Dasilva, J. J. R. F.; Herrmann, R.; Deus, N.; Castilho, T. J.; Silva, M. F. C. G., Redox Potential and Substituent Effects at Ferrocene Derivatives - Estimates of Hammett Sigma-P and Taft Polar Sigma Substituent Constants. *Journal of Organometallic Chemistry* **1991,** *421* (1), 75-90.
72. Roberts, R. M. G.; Silver, J., Mossbauer Studies on Ferrocene Complexes .12. Relationships between Oxidation Potentials and Quadrupole Splittings. *Journal of Organometallic Chemistry* **1984,** *263* (2), 235-241.

73. Sutherland, W., LXXV. A dynamical theory of diffusion for non-electrolytes and the molecular mass of albumin. *Philosophical Magazine Series 6* **1905,** *9* (54), 781-785.

74. Young, M. E.; Carroad, P. A.; Bell, R. L., Estimation of diffusion coefficients of proteins. *Biotechnology and Bioengineering* **1980,** *22* (5), 947-955.

75. Paddon, C. A.; Pritchard, G. J.; Thiemann, T.; Marken, F., Paired electrosynthesis: micro-flow cell processes with and without added electrolyte. *Electrochemistry Communications* **2002,** *4* (10), 825-831.

76. Guerrero, G.; Mutin, P. H.; Vioux, A., Anchoring of phosphonate and phosphinate coupling molecules on titania particles. *Chemistry of Materials* **2001,** *13* (11), 4367-4373.

77. Mutin, P. H.; Guerrero, G.; Vioux, A., Hybrid materials from organophosphorus coupling molecules. *Journal of Materials Chemistry* **2005,** *15* (35-36), 3761-3768.

78. Rusu, C. N.; Yates, J. T., Adsorption and decomposition of dimethyl methylphosphonate on TiO2. *Journal of Physical Chemistry B* **2000,** *104* (51), 12292-12298.

79. Mingalyov, P. G.; Lisichkin, G. V., Chemical modification of oxide surfaces with organophosphorus(v) acids and their esters. *Uspekhi Khimii* **2006,** *75* (6), 604-624.

80. Hotchkiss, P. J. The design, synthesis, and use of phosphonic aicds for the surface modification of metal oxides. Dissertation, Georgia Institute of Technology, 2008.

81. Giza, M.; Thissen, P.; Grundmeier, G., Adsorption kinetics of organophosphonic acids on plasma-modified oxide-covered aluminum surfaces. *Langmuir* **2008,** *24* (16), 8688-8694.

82. Langmuir, I., THE CONSTITUTION AND FUNDAMENTAL PROPERTIES OF SOLIDS AND LIQUIDS. PART I. SOLIDS. *Journal of the American Chemical Society* **1916,** *38* (11), 2221-2295.

83. Masel, R. I., *Principles of Adsorption and Reaction on Solid Surfaces*. Wiley Interscience: New York, 1996.

84. Dang, X.; Hupp, J. T., Luminescence-based assessment of thermodynamic constants for electrostatic binding of non-luminescent dyes and atomic ions to colloidal semiconductor surfaces. *Journal of Photochemistry and Photobiology A: Chemistry* **2001,** *143* (2â€“3), 251-256.

85. Raman, A.; Dubey, M.; Gouzman, I.; Gawalt, E. S., Formation of Self-Assembled Monolayers of Alkylphosphonic Acid on the Native Oxide Surface of SS316L. *Langmuir* **2006,** *22* (15), 6469-6472.

86. Paniagua, S. A.; Hotchkiss, P. J.; Jones, S. C.; Marder, S. R.; Mudalige, A.; Marrikar, F. S.; Pemberton, J. E.; Armstrong, N. R., Phosphonic acid modification of indium-tin oxide electrodes: Combined XPS/UPS/contact angle studies. *Journal of Physical Chemistry C* **2008,** *112* (21), 7809-7817.

87. Weng, Y.-X.; Li, L.; Liu, Y.; Wang, L.; Yang, G.-Z., Surface-Binding Forms of Carboxylic Groups on Nanoparticulate TiO2 Surface Studied by the Interface-Sensitive Transient Triplet-State Molecular Probe. *The Journal of Physical Chemistry B* **2003,** *107* (18), 4356-4363.

88. Li, H.; Paramonov, P.; Bredas, J. L., Theoretical study of the surface modification of indium tin oxide with trifluorophenyl phosphonic acid

molecules: impact of coverage density and binding geometry. *Journal of Materials Chemistry* **2010,** *20* (13), 2630-2637.

89. Shigesato, Y.; Paine, D. C., A microstructural study of low resistivity tin-doped indium oxide prepared by d.c. magnetron sputtering. *Thin Solid Films* **1994,** *238* (1), 44-50.

90. Yeom, H.-Y.; Popovich, N.; Chason, E.; Paine, D. C., A study of the effect of process oxygen on stress evolution in d.c. magnetron-deposited tin-doped indium oxide. *Thin Solid Films* **2002,** *411* (1), 17-22.

91. Gong, X.-Q.; Selloni, A.; Batzill, M.; Diebold, U., Steps on anatase TiO2(101). *Nat Mater* **2006,** *5* (8), 665-670.

92. Ji, S.-H.; Hannon, J. B.; Tromp, R. M.; Perebeinos, V.; Tersoff, J.; Ross, F. M., Atomic-scale transport in epitaxial graphene. *Nat Mater 11* (2), 114-119.

93. Dâ€™Souza, F.; Maligaspe, E.; Ohkubo, K.; Zandler, M. E.; Subbaiyan, N. K.; Fukuzumi, S., Photosynthetic Reaction Center Mimicry: Low Reorganization Energy Driven Charge Stabilization in Self-Assembled Cofacial Zinc Phthalocyanine Dimerâˆ’Fullerene Conjugate. *Journal of the American Chemical Society* **2009,** *131* (25), 8787-8797.

94. Norton, J. E.; Bredas, J. L., Theoretical characterization of titanyl phthalocyanine as a p-type organic semiconductor: Short intermolecular pi-pi interactions yield large electronic couplings and hole transport bandwidths. *Journal of Chemical Physics* **2008,** *128* (3).

95. Lin, H. C.; Polaske, N. W.; Oquendo, L. E.; Gliboff, M.; Knesting, K. M.; Nordlund, D.; Ginger, D. S.; Ratcliff, E. L.; Beam, B. M.; Armstrong, N. R.; McGrath, D. V.; Saavedra, S. S., Electron-Transfer Processes in Zinc Phthalocyanine Phosphonic Acid Monolayers on ITO: Characterization of Orientation and Charge-Transfer Kinetics by Waveguide Spectroelectrochemistry. *Journal of Physical Chemistry Letters* **2012,** *3* (9), 1154-1158.

96. Chen, H. N.; Ratner, M. A.; Schatz, G. C., Theoretical calculation of the photo-induced electron transfer rate between a gold atom and a gold cation solvated in CCl4. *Journal of Photochemistry and Photobiology a-Chemistry* **2011,** *221* (2-3), 143-147.

97. Marcus, R. A.; Sutin, N., Electron Transfers in Chemistry and Biology. *Biochimica Et Biophysica Acta* **1985,** *811* (3), 265-322.

98. Gray, H. B.; Winkler, J. R., Long-range electron transfer. *Proceedings of the National Academy of Sciences of the United States of America* **2005,** *102* (10), 3534-3539.

99. Persson, P.; Lundqvist, M. J.; Ernstorfer, R.; Goddard, W. A.; Willig, F., Quantum chemical calculations of the influence of anchor-cum-spacer groups on femtosecond electron transfer times in dye-sensitized semiconductor nanocrystals. *Journal of Chemical Theory and Computation* **2006,** *2* (2), 441-451.

100. Murray, R. W.; Ewing, A. G.; Durst, R. A., Chemically modified electrodes. Molecular design for electroanalysis. *Analytical Chemistry* **1987,** *59* (5), 379A-390A.

101. Marcus, R. A., Electrostatic Free Energy and Other Properties of States Having Nonequilibrium Polarization .1. *Journal of Chemical Physics* **1956,** *24* (5), 979-989.

102. Marcus, R. A., On the Theory of Oxidation-Reduction Reactions Involving Electron Transfer .1. *Journal of Chemical Physics* **1956,** *24* (5), 966-978.

103. Marcus, R. A., Chemical + Electrochemical Electron-Transfer Theory. *Annual Review of Physical Chemistry* **1964,** *15*, 155-&.

104. Chang, S.-C.; Shiao, M.-H., Smooth indium zinc oxide film prepared by sputtering a In2O3:ZnO=95:5 target. *Microelectronics Journal* **2007,** *38* (12), 1202-1206.

105. Kang, J. W.; Jeong, W. I.; Kim, J. J.; Kim, H. K.; Kim, D. G.; Lee, G. H., High-performance flexible organic light-emitting diodes using amorphous indium zinc oxide anode. *Electrochemical and Solid State Letters* **2007,** *10* (6), J75-J78.

106. Goncalves, G.; Grasso, V.; Barquinha, P.; Pereira, L.; Elamurugu, E.; Brignone, M.; Martins, R.; Lambertini, V.; Fortunato, E., Role of Room Temperature Sputtered High Conductive and High Transparent Indium Zinc Oxide Film Contacts on the Performance of Orange, Green, and Blue Organic Light Emitting Diodes. *Plasma Processes and Polymers* **2011,** *8* (4), 340-345.

107. Leenheer, A. J.; Perkins, J. D.; van Hest, M. F. A. M.; Berry, J. J.; Oâ€™Hayre, R. P.; Ginley, D. S., General mobility and carrier concentration relationship in transparent amorphous indium zinc oxide films. *Physical Review B* **2008,** *77* (11), 115215.

108. Akram Amooali Khosroabadi, P. G., Binh Au Thanh Duong, Jayan Thomas, Ajaya K. Sigdel, Joseph J. Berry, Thomas Gennet, N. Peyghambarian, Robert A. Norwood Fabrication, Electrical and Optical Properties of Silver, Indium substituted Tin and Zinc Oxide Nanostructure Arrays. *To be submitted for publication*.

109. Howell, J. O.; Wightman, R. M., Ultrafast Voltammetry and Voltammetry in Highly Resistive Solutions with Microvoltammetric Electrodes. *Analytical Chemistry* **1984,** *56* (3), 524-529.

110. Zhang, B.; Galusha, J.; Shiozawa, P. G.; Wang, G. L.; Bergren, A. J.; Jones, R. M.; White, R. J.; Ervin, E. N.; Cauley, C. C.; White, H. S., Bench-top method for fabricating glass-sealed nanodisk electrodes, glass nanopore electrodes, and glass nanopore membranes of controlled size. *Analytical Chemistry* **2007,** *79* (13), 4778-4787.

111. Gerischer, H., Electron-Transfer Kinetics of Redox Reactions at the Semiconductor Electrolyte Contact - a New Approach. *Journal of Physical Chemistry* **1991,** *95* (3), 1356-1359.

112. Gerischer, H.; Heller, A., The Role of Oxygen in Photooxidation of Organic-Molecules on Semiconductor Particles. *Journal of Physical Chemistry* **1991,** *95* (13), 5261-5267.

113. Lewis, N. S., An Analysis of Charge-Transfer Rate Constants for Semiconductor Liquid Interfaces. *Annual Review of Physical Chemistry* **1991,** *42*, 543-580.

114. Cline, K. K.; Mcdermott, M. T.; Mccreery, R. L., Anomalously Slow-Electron Transfer at Ordered Graphite-Electrodes - Influence of Electronic Factors and Reactive Sites. *Journal of Physical Chemistry* **1994,** *98* (20), 5314-5319.

115. Popovich, N. D.; Wong, S. S.; Yen, B. K. H.; Yeom, H. Y.; Paine, D. C., Influence of microstructure on the electrochemical performance of tin-doped indium oxide film electrodes. *Analytical Chemistry* **2002,** *74* (13), 3127-3133.

116. Moriga, T.; Okamoto, T.; Hiruta, K.; Fujiwara, A.; Nakabayashi, I.; Tominaga, K., Structures and Physical Properties of Films Deposited by Simultaneous DC Sputtering of ZnO and In2O3 or ITO Targets. *Journal of Solid State Chemistry* **2000,** *155* (2), 312-319.

117. Naghavi, N.; Marcel, C.; Dupont, L.; Rougier, A.; Leriche, J. B.; Guery, C., Structural and physical characterisation of transparent conducting pulsed laser deposited In2O3-ZnO thin films. *Journal of Materials Chemistry* **2000,** *10* (10), 2315-2319.

118. Tominaga, K.; Murayama, T.; Mori, I.; Okamoto, T.; Hiruta, K.; Moriga, T.; Nakabayashi, I., Conductive transparent films deposited by simultaneous sputtering of zinc-oxide and indium-oxide targets. *Vacuum* **2000,** *59* (2â€“3), 546-552.

119. Jung, Y. S.; Seo, H. Y.; Lee, D. W.; Jeon, D. Y., Influence of DC magnetron sputtering parameters on the properties of amorphous indium zinc oxide thin film. *Thin Solid Films* **2003,** *445* (1), 63-71.

120. Matthew Gliboff, L. S., Kristina M. Knesting, Mattew C. Schalnat, Anoma Mudalige, Erin L. Ratcliff, Hong Li, Ajaya K. Sigdel, Joseph J. Berry, Dennis Nordlund, Anthony J. Giordano, Gerald T. Seidler, Jean-Luc Bredas, Seth R. Marder, Jeanne E. Pemberton, David S. Ginger, Orientation and Order of Phenylphosphonic Acid Self-assembled Monolayers on Transparent Conductive Oxides: A Combined NEXAFS, PM-IRRAS and DFT Study. *Submitted to Journal of the American Chemical Society* **2012**.

121. Manzhos, S.; Segawa, H.; Yamashita, K., The effect of ligand substitution and water co-adsorption on the adsorption dynamics and energy level matching of amino-phenyl acid dyes on TiO2. *Physical Chemistry Chemical Physics* **2012,** *14* (5), 1749-1755.

122. Nicholso.Rs, Theory and Application of Cyclic Voltammetry for Measurement of Electrode Reaction Kinetics. *Analytical Chemistry* **1965,** *37* (11), 1351-&.

123. Laviron, E., General Expression of the Linear Potential Sweep Voltammogram in the Case of Diffusionless Electrochemical Systems. *Journal of Electroanalytical Chemistry* **1979,** *101* (1), 19-28.